

DEVELOPMENT AND VALIDATION OF AN  
INTERACTIVE REMOTE PHYSICAL THERAPY SYSTEM

---

A Thesis  
presented to  
the Faculty of the Graduate School  
at the University of Missouri-Columbia

---

In Partial Fulfillment  
of the Requirements for the Degree  
Master of Science

---

by  
ANUP KUMAR MISHRA  
Dr. Marjorie Skubic, Thesis Advisor

MAY 2015

The undersigned, appointed by the dean of the Graduate School, have examined the thesis entitled

DEVELOPMENT AND VALIDATION OF AN  
INTERACTIVE REMOTE PHYSICAL THERAPY SYSTEM

presented by Anup Kumar Mishra,

a candidate for the degree of Master of Science,

and hereby certify that, in their opinion, it is worthy of acceptance.

---

Dr. Marjorie Skubic, Professor, Dept. of Electrical and  
Computer Engineering and Dept. of Computer Science

---

Dr. James Keller, Curators Professor, Dept. of Electrical  
and Computer Engineering and Dept. of Computer  
Science

---

Dr. Carmen Abbott, Clinical Professor, Dept. of Physical  
Therapy, School of Health Professions

To Mama and Daddy...

## ACKNOWLEDGEMENTS

I would like to gratefully thank Dr. Marjorie Skubic, my adviser, for her guidance, invaluable constructive criticism and friendly advice during this research work. I am sincerely grateful to her for sharing her truthful and illuminating views on a number of issues related to this work.

I would like to sincerely thank the members of my thesis committee, Dr. James Keller and Dr. Carmen Abbott, for their input and valuable suggestions to further improve my research work.

I would also like to express my gratitude to everyone who supported me throughout my research. I owe deepest gratitude to my parents and family members. Without their motivation, faith, and continuous support this would not have been possible.

I am very grateful to my friends, especially, Shradha Shalini, Piyush P. Khopkar, Nakul Khadilkar, and Tushar K. Das for their insight and help during my studies. I am also thankful to my lab members for their support in Center for Eldercare and Rehabilitation Technology lab.

## Table of Contents

ACKNOWLEDGEMENTS.....	ii
List of Figures .....	vii
List of Tables .....	xi
Abstract.....	xiii
Chapter 1.....	1
Introduction .....	1
Motivation .....	1
Problem Statement.....	3
Primary Goals.....	5
Contributions of this thesis.....	5
Chapter 2.....	7
Background .....	7
Review: Sensor based Physical Rehabilitation Systems.....	7
Kinect-Based Rehabilitation Systems.....	7
Postural Balance Assessments using Force Plate System.....	10
Chapter 3.....	15
System Overview .....	15
Sensors and Equipment .....	15
Microsoft Kinect Sensors .....	15

Vicon Motion Capture System .....	17
NeuroCom System .....	17
Interactive Interfaces for Remote PT .....	18
Challenges .....	24
Chapter 4.....	26
Methodology.....	26
Biomechanical Features.....	26
Trunk Sway .....	26
Joint Alignments.....	28
Single Leg Stance Time Period .....	28
Full Body Center of Mass (CoM) .....	29
CoG and CoM plots .....	36
Postural Sway Angle (deg) .....	37
Sway velocity (deg/sec).....	39
Step width (cm).....	40
Speed (cm/sec) .....	41
End Sway (deg/sec) .....	42
AP and ML Sway Range (cm).....	42
Validation Methods .....	43
Validation with the Vicon System .....	43

Validation of Full-Body CoM measurements .....	44
Validation with the NeuroCom System.....	44
Chapter 5.....	47
Results and Discussion .....	47
Trunk Sway Validation with the Vicon System .....	47
Full-Body CoM measurement comparison with the Vicon and Forceplate system .....	48
Validation with the NeuroCom System .....	49
NeuroCom validation Results .....	50
The NeuroCom Classification Accuracy .....	55
Therapist’s Ratings Compilation .....	59
Chapter 6.....	62
Conclusion.....	62
Contribution.....	62
Limitation of the Study .....	63
Future Work.....	65
Bibliography .....	67
Appendix A.....	71
CoG and CoM traces for NeuroCom validation test .....	71
Test results for Subject 1 .....	72
Test results for Subject 2 .....	76

Test results for Subject 3 .....	80
Test results for Subject 4 .....	84
Appendix B.....	88
Code and Data Repository .....	88

## List of Figures

Figure 1 VR Solutions for Physical Therapy; taken from[11]. .....	8
Figure 2 Sample report of NeuroCom unilateral stance assessment; taken from [34]. .....	12
Figure 3 Sample report of NeuroCom TW assessment; taken from [34]. .....	13
Figure 4 (a): Xbox 360 Kinect (K1); (b): Xbox One Kinect (K2); (c, e): K1 depth image with skeleton overlay on a human body segment for single leg stance and tandem walk; (d, f): K2 depth image with skeleton overlay on a human body segment for single leg stance. ....	16
Figure 5 A subject performing US on a NeuroCom System; taken from [34]. .....	18
Figure 6 (a): Therapist’s application (b): PT client’s application .....	20
Figure 7 Block Diagram of IPTS. ....	23
Figure 8 Result window showing SLS post-activity data. ....	23
Figure 9 Result window showing TW post-activity data. ....	24
Figure 10 (left): Trunk Sway in AP direction; (right) Trunk Sway in ML direction.....	27
Figure 11 Body Segments for GEBOD III regression equations [51]. ....	29
Figure 12 Single leg stance plots: (a): CoG plot from NeuroCom; (b) CoM plot from K1; (c): CoM plot from K2. ....	37
Figure 13 Tandem walk plots: (a): CoG plot from NeuroCom; (b) CoM plot from the K1; (c): CoM plot from the K2. ....	37
Figure 14 Sway Angle Representation. ....	38
Figure 15 Sway vector angle representation ( $\theta_{Ch}$ ). ....	39
Figure 16 (Front view of Tandem Walk) Step width representation (W). ....	41
Figure 17 AP and ML Sway Range .....	42
Figure 18 AP and ML trunk sway axis with respect to global coordinates of K1, K2, and Vicon. ...	44

Figure 19 Subject performing SLS for the NeuroCom, K1, and K2 validation..... 45

Figure 20 Skeletal model of subject while performing TW by (a): K1; (b): K2 SDKs. The blue ring in each image shows the distorted skeletal joints..... 52

Figure 21 SLS (a): CoG plot by NeuroCom; SLS CoM plot by (b): K1; (c): K2; TW (d): CoG plot by NeuroCom; TW CoM plot by (e): K1; (f): K2..... 55

Figure 22 Classification accuracy for K1 and K2 sensors in measuring Sway Velocity, Step Width, Speed, and End Sway. .... 58

Figure 23 Technical Quality of Audio and Video: using Remote PT Application (rated 1/poor to 5/excellent). .... 60

Figure 24 User satisfaction and PT interaction: using remote PT application (rated 1/disagree to 5/agree). .... 61

Figure 25 Subject 1- SLS eyes open test results. Trial 1: (a) NeuroCom CoG plot; (b) K1 CoM plot; (c) K2 CoM plot; Trial 2: (d) NeuroCom CoG plot; (e) K1 CoM plot; (f) K2 CoM plot; Trial 3: (g) NeuroCom CoG plot; (h) K1 CoM plot; (i) K2 CoM plot. .... 72

Figure 26 Subject 1- SLS eyes closed test results. Trial 1: (a) NeuroCom CoG plot; (b) K1 CoM plot; (c) K2 CoM plot; Trial 2: (d) NeuroCom CoG plot; (e) K1 CoM plot; (f) K2 CoM plot; Trial 3: (g) NeuroCom CoG plot; (h) K1 CoM plot; (i) K2 CoM plot. .... 73

Figure 27 Subject 1- TW eyes open test results. Trial 1: (a) NeuroCom CoG plot; (b) K1 CoM plot; (c) K2 CoM plot; Trial 2: (d) NeuroCom CoG plot; (e) K1 CoM plot; (f) K2 CoM plot; Trial 3: (g) NeuroCom CoG plot; (h) K1 CoM plot; (i) K2 CoM plot. .... 74

Figure 28 Subject 1- TW eyes closed test results. Trial 1: (a) NeuroCom CoG plot; (b) K1 CoM plot; (c) K2 CoM plot; Trial 2: (d) NeuroCom CoG plot; (e) K1 CoM plot; (f) K2 CoM plot; Trial 3: (g) NeuroCom CoG plot; (h) K1 CoM plot; (i) K2 CoM plot. .... 75

Figure 29 Subject 2- SLS eyes open test results. Trial 1: (a) NeuroCom CoG plot; (b) K1 CoM plot; (c) K2 CoM plot; Trial 2: (d) NeuroCom CoG plot; (e) K1 CoM plot; (f) K2 CoM plot; Trial 3: (g) NeuroCom CoG plot; (h) K1 CoM plot; (i) K2 CoM plot. .... 76

Figure 30 Subject 2- SLS eyes closed test results. Trial 1: (a) NeuroCom CoG plot; (b) K1 CoM plot; (c) K2 CoM plot; Trial 2: (d) NeuroCom CoG plot; (e) K1 CoM plot; (f) K2 CoM plot; Trial 3: (g) NeuroCom CoG plot; (h) K1 CoM plot; (i) K2 CoM plot. .... 77

Figure 31 Subject 2- TW eyes open test results. Trial 1: (a) NeuroCom CoG plot; (b) K1 CoM plot; (c) K2 CoM plot; Trial 2: (d) NeuroCom CoG plot; (e) K1 CoM plot; (f) K2 CoM plot; Trial 3: (g) NeuroCom CoG plot; (h) K1 CoM plot; (i) K2 CoM plot. .... 78

Figure 32 Subject 2- TW eyes closed test results. Trial 1: (a) NeuroCom CoG plot; (b) K1 CoM plot; (c) K2 CoM plot; Trial 2: (d) NeuroCom CoG plot; (e) K1 CoM plot; (f) K2 CoM plot; Trial 3: (g) NeuroCom CoG plot; (h) K1 CoM plot; (i) K2 CoM plot. .... 79

Figure 33 Subject 3- SLS eyes open test results. Trial 1: (a) NeuroCom CoG plot; (b) K1 CoM plot; (c) K2 CoM plot; Trial 2: (d) NeuroCom CoG plot; (e) K1 CoM plot; (f) K2 CoM plot; Trial 3: (g) NeuroCom CoG plot; (h) K1 CoM plot; (i) K2 CoM plot. .... 80

Figure 34 Subject 3- SLS eyes closed test results. Trial 1: (a) NeuroCom CoG plot; (b) K1 CoM plot; (c) K2 CoM plot; Trial 2: (d) NeuroCom CoG plot; (e) K1 CoM plot; (f) K2 CoM plot; Trial 3: (g) NeuroCom CoG plot; (h) K1 CoM plot; (i) K2 CoM plot. .... 81

Figure 35 Subject 3- TW eyes open test results. Trial 1: (a) NeuroCom CoG plot; (b) K1 CoM plot; (c) K2 CoM plot; Trial 2: (d) NeuroCom CoG plot; (e) K1 CoM plot; (f) K2 CoM plot; Trial 3: (g) NeuroCom CoG plot; (h) K1 CoM plot; (i) K2 CoM plot. .... 82

Figure 36 Subject 3- TW eyes closed test results. Trial 1: (a) NeuroCom CoG plot; (b) K1 CoM plot; (c) K2 CoM plot; Trial 2: (d) NeuroCom CoG plot; (e) K1 CoM plot; (f) K2 CoM plot; Trial 3: (g) NeuroCom CoG plot; (h) K1 CoM plot; (i) K2 CoM plot. .... 83

Figure 37 Subject 4- SLS eyes open test results. Trial 1: (a) NeuroCom CoG plot; (b) K1 CoM plot; (c) K2 CoM plot; Trial 2: (d) NeuroCom CoG plot; (e) K1 CoM plot; (f) K2 CoM plot; Trial 3: (g) NeuroCom CoG plot; (h) K1 CoM plot; (i) K2 CoM plot. .... 84

Figure 38 Subject 4- SLS eyes closed test results. Trial 1: (a) NeuroCom CoG plot; (b) K1 CoM plot; (c) K2 CoM plot; Trial 2: (d) NeuroCom CoG plot; (e) K1 CoM plot; (f) K2 CoM plot; Trial 3: (g) NeuroCom CoG plot; (h) K1 CoM plot; (i) K2 CoM plot. .... 85

Figure 39 Subject 4- TW eyes open test results. Trial 1: (a) NeuroCom CoG plot; (b) K1 CoM plot; (c) K2 CoM plot; Trial 2: (d) NeuroCom CoG plot; (e) K1 CoM plot; (f) K2 CoM plot; Trial 3: (g) NeuroCom CoG plot; (h) K1 CoM plot; (i) K2 CoM plot. .... 86

Figure 40 Subject 4- TW eyes closed test results. Trial 1: (a) NeuroCom CoG plot; (b) K1 CoM plot; (c) K2 CoM plot; Trial 2: (d) NeuroCom CoG plot; (e) K1 CoM plot; (f) K2 CoM plot; Trial 3: (g) NeuroCom CoG plot; (h) K1 CoM plot; (i) K2 CoM plot. .... 87

## List of Tables

Table 1 SEGMENT CENTERS FOR K1.....	33
Table 2 SEGMENT CENTERS FOR K2.....	34
Table 3 TRUNK SWAY ANGLE DEVIATION FOR THE SINGLE LEG STANCE TEST COMPARED TO THE VICON.....	47
Table 4 TRUNK SWAY ANGLE DEVIATION FOR THE TANDEM WALK TEST COMPARED TO THE VICON.....	48
Table 5 SWAY RANGE DEVIATION FOR THE SINGLE LEG STANCE TEST COMPARED TO THE VICON AND FORCEPLATE.....	49
Table 6 SWAY VELOCITY DEVIATION FOR THE SINGLE LEG STANCE TEST COMPARED TO THE NEUROCOM .....	50
Table 7 STEP WIDTH DEVIATION FOR THE TANDEM WALK TEST COMPARED TO THE NEUROCOM .....	51
Table 8 STEP WIDTH DEVIATION FOR THE TANDEM WALK TEST COMPARED TO THE NEUROCOM WITH OUT CONSIDERING DEVIATIONS OF SUBJECT 3.....	51
Table 9 SPEED DEVIATION FOR THE TANDEM WALK TEST COMPARED TO THE NEUROCOM: Using CoM Method.....	52
Table 10 SPEED DEVIATION FOR THE TANDEM WALK TEST COMPARED TO THE NEUROCOM: Using Spinal Joint Alone.....	53
Table 11 END SWAY DEVIATION FOR THE TANDEM WALK TEST COMPARED TO THE NEUROCOM .....	54
Table 12 CLASSIFICATION OF MEAN COM SWAY VELOCITES COMPARED TO THE NEUROCOM ..	56
Table 13 CLASSIFICATION OF STEP WIDTH COMPARED TO THE NEUROCOM .....	56

Table 14 CLASSIFICATION OF SPEED COMPARED TO THE NEUROCOM ..... 57

Table 15 CLASSIFICATION OF END SWAY COMPARED TO THE NEUROCOM ..... 58

## Abstract

We present an Interactive Physical Therapy System (IPTS) for remote quantitative assessment of clients in the home. The system consists of two different interactive interfaces connected through a network, for a real-time low latency video conference using audio, video, skeletal, and depth data streams from a Microsoft Kinect. To test the potential of IPTS, experiments were conducted with 5 independent living senior subjects in Kansas City, MO. Also, experiments were conducted in the lab to validate the real-time biomechanical measures calculated using the skeletal data from the Microsoft Xbox 360 Kinect and Microsoft Xbox One Kinect, with ground truth data from a Vicon motion capture system and a NeuroCom forceplate system. Good agreements were found in most of the validation tests. The results show potential capabilities of the IPTS system to provide remote physical therapy to clients, especially older adults, who may find it difficult to visit the clinic.

## Chapter 1

### Introduction

This chapter provides an overview of the motivation, problem statement, and primary goals of the Kinect based *Interactive Physical Therapy System (IPTS)*.

### Motivation

Physical Therapy (PT) is a major rehabilitation methodology to improve postural control and functional abilities. A study in 2009 showed only 6.2 physical therapists per 10,000 people across the United States [1]. Many PT clients, especially older adults, may have a hard time getting to the clinic due to distance or logistics (e.g., rural residents and those in large cities). Particularly in the case of eldercare, PT services can be proactively delivered from remote clinic sites to allow unobtrusive, continuous monitoring and personalized coaching in the homes of PT clients [2-5]. Given the challenges faced in providing physical therapy services due to limited facilities and human resources, a new class of smart tele-health systems is proposed to deliver quality and faster services [6-8]. A tele-health system can help with early interventions, better health outcome with fewer clinical visits, and faster one-on-one interactive care. With Gigabit networking becoming economically feasible and widely installed in homes through city-supported programs such as Google Fiber in several US cities such as Kansas City, there are new opportunities to

revisit in-home, personalized tele-health services. The opportunities include the conceptualization and implementation of Gigabit applications that use the latest advances in sensing, high-definition video-based communication, and cloud computing. The Gigabit applications within novel tele-health service compositions can enable: early interventions, better health outcomes through fewer hospital visits, better one-on-one interactive care, and ultimately significant cost savings in the relatively expensive eldercare health market sector.

In the diverse field of healthcare, novel tele-health services in the context of “Physical Therapy” are particularly attractive for both the therapists and PT clients. We introduce an interactive remote PT system that helps the PT clients to “see” the therapist more frequently so they can be assessed more frequently, get their exercises updated if necessary, and make sure they are performing them correctly with real-time feedback from the therapist. Also, not all clinics have the expensive commercial PT equipment, such as NeuroCom, ArcGIS Pipeline Data Model (APDM) systems for balance assessment and not everyone has access to them because of scheduling issues. So with the use of this proposed application, more people will have easier access to quantitative measurement of their gait and balance.

The system design and components of the service leverage a high-speed, low-latency network connection through an interactive interface built on top of the Microsoft Kinect motion sensing capabilities. We utilized the openly available Kinect Software Development Kit (Kinect SDK 1.8), C# language and Windows Presentation Foundation (WPF) technologies on .Net Framework 4.5 in our interactive interface development environment.

Two separate interface variants have been developed, one for the therapist side, and another for the PT client side, in order to address the unique needs of the interaction (e.g., the therapist can use voice commands) and exercise assessment (e.g., the therapist can generate exercise activity reports for discussion with the PT client).

The Interactive Physical Therapy System (IPTS) uses the Kinect sensors to establish a live audio-video communication between the therapist and PT client, with detailed real-time analysis of joint alignments and trunk sway from the skeletal data of the client in the home. A post-activity result window provides a trace of L5 motion in the horizontal plane, maximum trunk sway values in anteroposterior (AP) and mediolateral (ML) directions for Single Leg Stance (SLS) and Tandem Walk (TW), with eyes open and eyes closed tests. A Vicon motion capture system was used for ground truth comparison. Also, the Microsoft Xbox 360 Kinect (K1) was compared with the recently introduced Microsoft Xbox One Kinect (K2) to verify the stability and accuracy of both with respect to the Vicon system. The IPTS system built using user-centered design principles for in-home PT coaching is more than a typical videoconferencing application. It integrates 2D video feeds between the therapist and PT client along with 3D sensing data to provide an immersive experience.

### Problem Statement

There are many gold standard conventional PT systems those have been used for the assessment of body balance, such as, the NeuroCom Systems, the APDM accelerometers, and the Vicon motion capture systems [9]. Neither of these systems are readily available in many small PT clinics around the globe nor are they very user friendly.

Also, they are not very comfortable to use because of the wearable technology involved in them, e.g., accelerometers in the APDM system and reflection markers in the Vicon system. Expense of these systems is an issue as well.

Considering the above problems, many researchers came up with different solutions, including the Kinect sensor-based rehabilitation technologies. Most Kinect-based therapy and rehabilitation systems use a gamification or virtual reality technology [10-16] for activity assessments. These systems are efficient but do not involve a physical therapist to help the PT client with proper guidance. There has to be an individualistic approach to assess people with critical balance issues and injuries. An in-person communication with the therapist would definitely help the PT clients to understand the assessments better. However, as mentioned above, it can be difficult for an older adult to travel from their community to a physical therapy center. In this study, we introduce the IPTS system to address all these issues by providing remote physical therapy over a network in real-time.

The IPTS is highly dependent on network conditions. More specifically, a therapist needs to be able to confidently assess whether non-ideal performance in the physical therapy activities of a PT client is being impacted due to lag in network communications for the data-intensive interactive session, or in fact are due to the physical and cognitive limitations of the PT client. To address this problem we came up with an analytics approach that involves a network quality estimation module whose output provides visual evidence to the PT client and therapist regarding any undesirable network status that degrade user experience and may cause any exercise mis-assessment.

## Primary Goals

The primary goals of this study are:

- To develop two unique interactive applications (one for the therapist with quantitative assessment of gait and balance, and another for the PT client) using *Iterative design* principles [17, 18], and *User-centered design* [19, 20] methodology.
- To integrate a suitable network service for better Kinect data (audio, RGB video, skeletal, and depth) communication between the two applications with minimal or no data loss and delay.
- Comparing assessment results from an IPTS using Xbox 360 Kinect (K1: that uses Kinect SDK 1.8) with an IPTS using Xbox One Kinect (K2: that uses Kinect SDK 2.0) and validating those results with the Gold Standard PT assessment systems, such as, the NeuroCom system, and the Vicon system.

## Contributions of this thesis

In this thesis, we address the problems related to conventional in-clinic PT, by providing a next generation interactive remote PT system that has potential capabilities to provide remote physical therapy to clients, especially older adults, who may find it difficult to visit the clinic. The other contributions are the comparison studies conducted to validate the real-time biomechanical measures calculated using the skeletal data from the Microsoft Xbox 360 Kinect and Microsoft Xbox One Kinect, with ground truth data from a Vicon

motion capture system and NeuroCom long force-plate system. Our fourth contribution in this study is the evaluation of the usability of IPTS in real world scenarios. Experiments were conducted with five independent living older adults in Kansas City, MO and the therapist in Columbia, MO.

The remainder of this thesis is structured as follows. In chapter 2, we present a literature review of a few Kinect-based PT systems, followed by a description about clinical postural balance assessment systems using force-plates. In chapter 3, we show the difference between the two Kinect sensors and their SDKs, how the Vicon motion capture system and NeuroCom force-plate systems work, followed by a detailed description about the proposed interactive remote PT system. In chapter 4, we present the different biomechanical measures produced by the IPTS during real-time and post-activity data analysis, followed by the validation methodologies used to validate the Kinect sensor-based results with the Vicon system and the NeuroCom system. Then, we present the results of each validation study conducted with a detailed analysis in chapter 5. Finally, chapter 6 provides a description of the key contributions of this thesis, followed by a conclusion and future work.

## Chapter 2

### Background

This chapter provides a review of the existing sensor based rehabilitation systems and the gold standard PT assessment tools.

#### Review: Sensor based Physical Rehabilitation Systems

There have been earlier studies relating to developing sensor-based remote physical therapy and other exercise systems. In this section some of the most relevant systems based on Kinect sensor and accelerometers will be reviewed.

#### Kinect-Based Rehabilitation Systems

There have been a number of studies determining the accuracy of depth images and skeletal model provided by the Kinect in various fields [21-23] and for assessment of postural control [24, 25]. In [11], the authors designed two different Virtual Reality (VR) applications using the Vicon and Kinect technologies, for both local and remote physical therapy. They create Avatars of the PT client and the therapist in real-time within the applications, and the communications between the PT client and therapist is through each other's Avatar models. The therapist and PT client would see each other's Avatars and not the real persons, and they are dependent only on the skeletal data. This can be confusing

and not as beneficial as a real-time video conferencing. The Fig. 1 shows a Kinect-based setup (left) and another Vicon-based setup (right) with people and their Avatars on the screen.

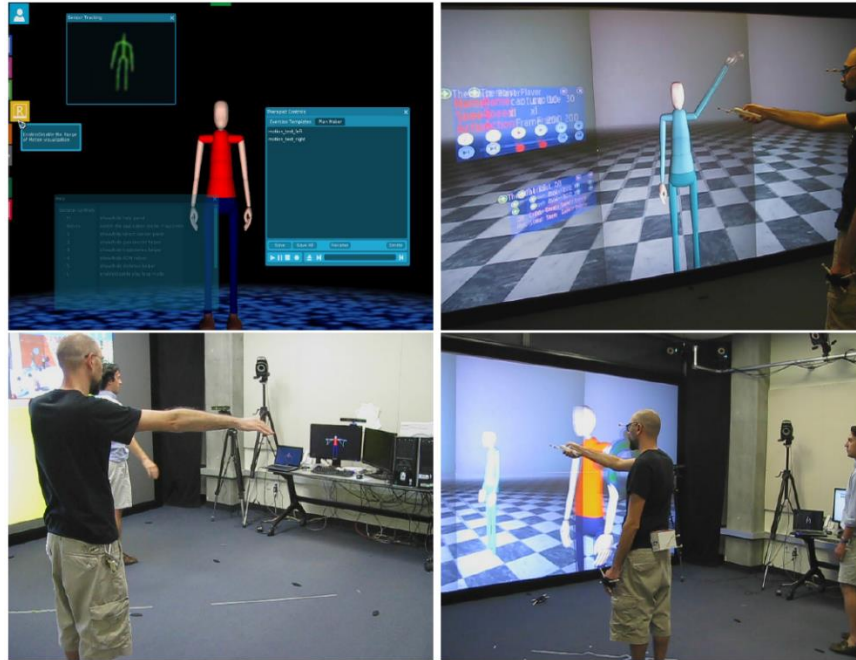


Figure 1 VR Solutions for Physical Therapy; taken from[11].

In another related study [8], the authors use a motion capture application for remote orthopedics rehabilitation. This system uses a set of gaming motion capture technologies (e.g., Wii, Kinect, and PlayStation Move) for exercise data collection in different scenarios involving clinic and home sites. In their remote sessions, the exercise data is not exchanged in real-time through a videoconferencing setup, but is sent over a network for offline visualization and feedback. The offline nature was pertinent in their case given the purpose of their application was to allow the PT client to learn how to perform exercises correctly at the clinic, and later execute them at their home without any therapist by their side.

PhysioMate [13], is a similar Virtual Reality (VR)-based system, specially designed for people using wheel chairs, for rehabilitation and exercises related to their upper body movements. Erdenetsogt et al. in [10] provides another example of a game-based VR systems for rehabilitation that uses a set of activities and analyze the accuracy measure of each activity.

Makawat et al. introduced an interesting concept of self-physical rehabilitation [12] using the Kinect sensor. The system uses a VR system to provide training to a PT client about 9 different PT activities including Side Leg Raise, Tandem Walk, and Timed UP and GO. The manual analysis of the system shows good accuracy of the algorithms. But the system is always used as a local VR model that does not send or receive any data to the actual physical therapist. The activities are not monitored by the therapist in real-time or post-exercise.

Some other Kinect-based gamification studies include [14-16]. They are again VR systems with different gamification strategies for rehabilitation. In [15], Davud et al. developed a motion-based tactile rendering algorithm for upper-limb. They use Haptic Gloves to provide feedback to the PT client through vibration. They designed three different games like the Wiping table game, Meteor Game, and Rope Game to train the PT client with these daily life activities and evaluate his/her performance.

Other Kinect-based works that have been investigated include exercise coaching with vision through a socially assistive robot coach [26], pre-recorded videos with automated coaching advice [27], the Wiimotes attached to limbs for movement-training exercises [28], and wearable sensing with iPods for tracking home balance exercises [29].

All these Kinect-based systems help in rehabilitation but they cannot replace in-person therapy by a physical therapist. These systems may help people with minor injuries but people with worse injuries may find them difficult to use. The IPTS is basically a video conferencing application using the Kinect. A physical therapist can communicate with the PT client through video and audio communication, and can also see the real-time analysis of gait and balance on the same application.

### Postural Balance Assessments using Force Plate System

There have been many studies related to human postural balance and sway and how aging and other physical impairments effect it [30, 31]. The human postural control system works as a feedback control circuit between the brain and the muscle and skeletal system. The muscles of the lower body and truncus, using this system, allows the individual to stand straight against the gravitational force [32]. Many different assessment techniques are used to obtain postural balance. Advancements in technology have provided the PT community with systems, such as forceplate and accelerometer-based systems for quantitatively assessing balance and gait. These systems provide highly accurate method of quantitatively assess postural balance through analysis of postural sway. Some important aspects of postural control evaluated by force platforms are: steadiness, symmetry, and dynamic stability. Steadiness is the proficiency of keeping the body motionless, which is considered as an important measure of postural sway. Whereas, symmetry is about an equal distribution of body weight between the feet while standing straight, which is a measure of Center of Pressure (CoP). Ability of moving the vertical projection of the Center of Gravity (CoG) around a supporting base is called the dynamic stability of human body [33].

NeuroCom is a forceplate-based system. The NeuroCom provides a set of assessment protocols to quantify the balance impairments of a PT client. In this study, we used the long forceplate platform of NeuroCom for two of the functional limitation assessments, such as Unilateral Stance (US) and Tandem Walk (TW) tests [34]. Both these tests provide a CoG trace of the activity trial. The US quantifies postural sway velocity with the PT client standing on either the right or left foot on the forceplate, with eyes open and with eyes closed. The length of each trial is ten seconds. The US test is very sensitive. Also, the US considers a large number of independent factors that can impact the PT client's performance.

Fig. 2 shows a sample report of US assessment. A CoG trace of each trial in both eyes open and eyes closed trials are displayed at the top of the results page. A graphical color coded representation of mean CoG sway velocities for each test is displayed at the bottom. These bars represent the CoG stability of the PT client during the assessment. There is also a center bar graph that represents the percentage difference score.

The gray color shaded area in the graphs represents the performance outside the normal data range, color coding each graph as red. Green color code represents a more stable performance within the normal data range. Each graph is represented with a numerical value at the top indicating the quantitative measurement.

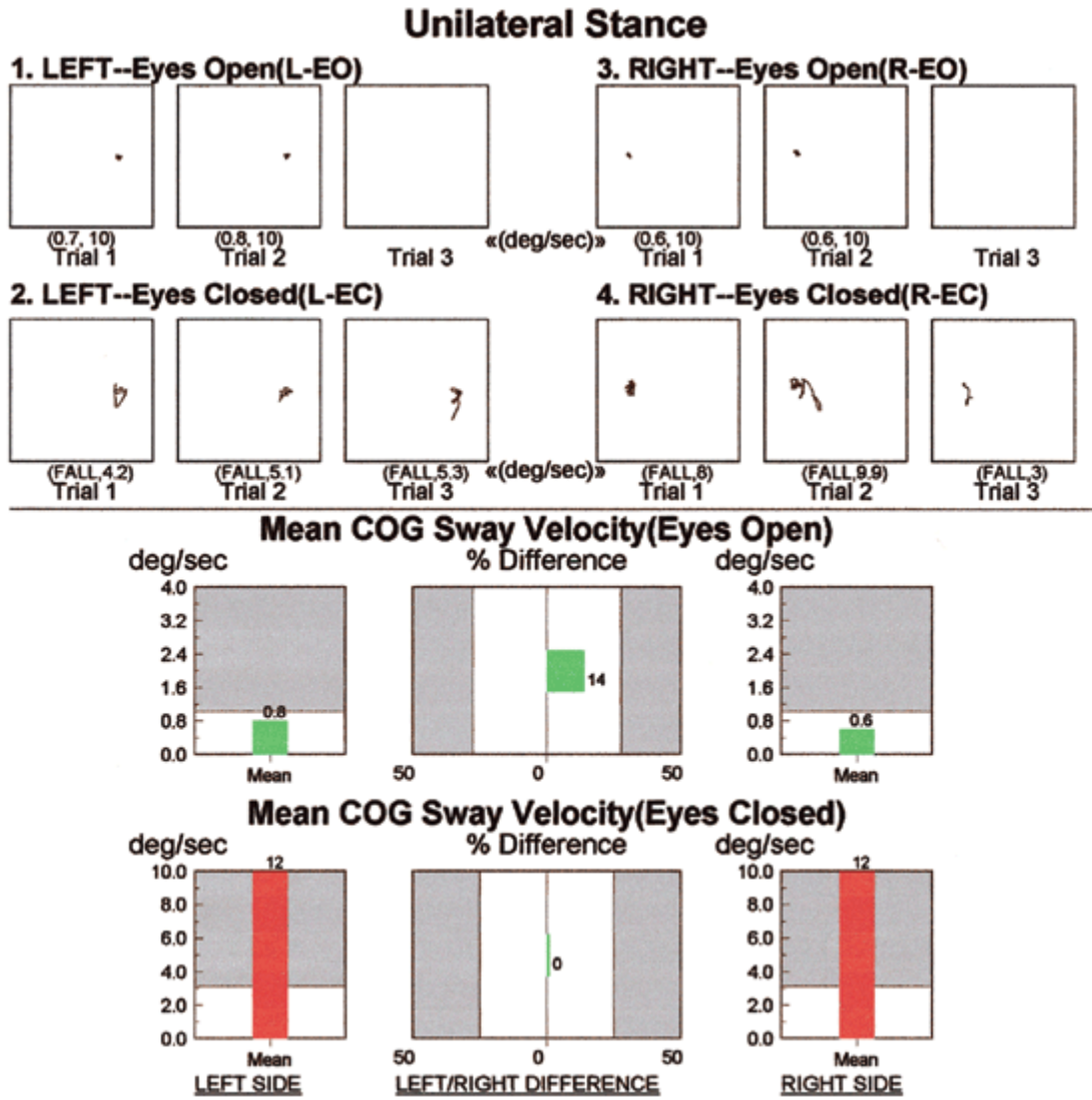


Figure 2 Sample report of NeuroCom unilateral stance assessment; taken from [34].

The quantitative measurements of unilateral stance assessments are based on a number of research studies done on postural balance assessments using force plate systems [35-37].

The TW test provides a gait analysis as the PT client walks heel to toe from one end of the long forceplate to the other end. This test measures three parameters, such as, step width, speed, and endpoint sway velocity [34]. Fig. 3 shows a sample report generated by NeuroCom for the TW test.

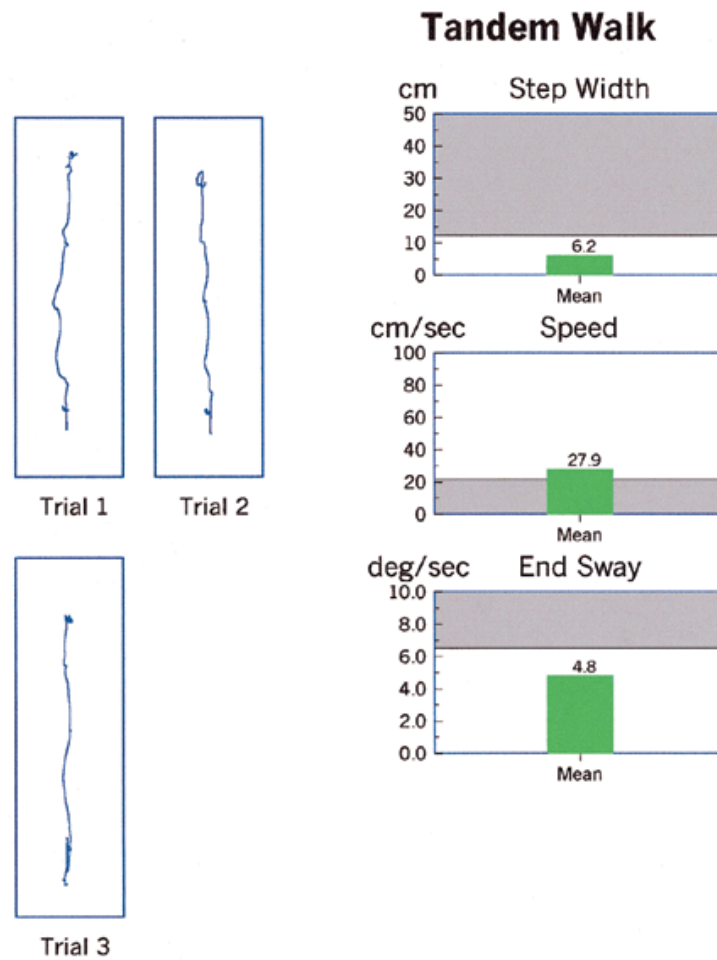


Figure 3 Sample report of NeuroCom TW assessment; taken from [34].

Similar to US, TW assessment report also provides a CoG trace of the walk performed by the PT client on the NeuroCom force plates. The report also provides quantitative measurements including the step width, speed of forward walk, and the velocity in degree per second of AP component of CoG sway for 5 seconds starting when the PT client terminates walking i.e. end sway. The quantitative measurements of TW assessment is also based on a number of research studies done on postural balance assessments using force plate system [38-40].

The color coded classification results provide a straightforward visualization of postural balance of the PT client. The simplicity and high accuracy of the NeuroCom system makes it the gold standard PT assessment equipment. The NeuroCom comes at a steep price of \$250,000, which makes it less affordable for many PT centers and hospitals around the globe [41].

## Chapter 3

### System Overview

This chapter provides a brief description about the sensors and techniques used for development of the Interactive PT System and its validation.

#### Sensors and Equipment

##### Microsoft Kinect Sensors

The K1 and K2 Kinect sensors, shown in Fig. 4 (a) and (b), are two widely used inexpensive depth sensors for motion analysis. Kinect K1 uses an infrared sensitive camera that generates a depth image from a pattern of actively emitted infrared light. Kinect K2 uses a time-of-flight phase detection camera system to get the depth image [42]. They both generate depth images independent of ambient lighting. The Kinect Software Development Kit 1.8 for K1 and 2.0 for K2 provided by Microsoft help in fitting 20 point and 25 point skeletal models, respectively, to segmented human bodies [43, 44]. Skeletal models generated by both systems are shown in Fig. 4 (c), (d), (e), and (f). In this study, we investigate the K1 and K2 Kinects and evaluate the accuracy and stability of trunk sway measured by each system.



(a)



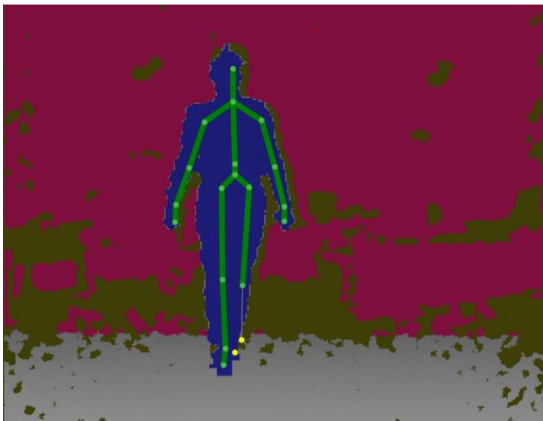
(b)



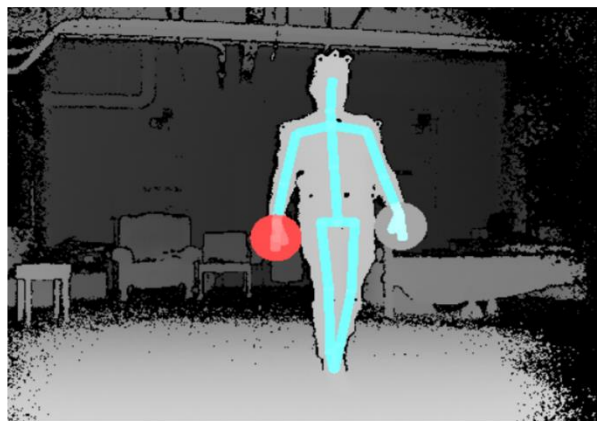
(c)



(d)



(e)



(f)

Figure 4 (a): Xbox 360 Kinect (K1); (b): Xbox One Kinect (K2); (c, e): K1 depth image with skeleton overlay on a human body segment for single leg stance and tandem walk; (d, f): K2 depth image with skeleton overlay on a human body segment for single leg stance.

## Vicon Motion Capture System

The Vicon motion capture system is an infrared marker-based motion capture system that provides high resolution of 3D spatial displacements. The system uses multiple cameras to monitor human motion. Initially, the system calibrates all the cameras to a common reference plane. Then, the reference plane calibrates to a global coordinate plane, which is referenced in Visual 3D. The nexus software package helps in calibrating the plane and acquiring 3D data from the reflective markers on human subjects. The system has accuracy of 0.5 mm and a sampling rate of 100 Hz [45, 46]. The Vicon system in the motion capture lab at Center for Eldercare and Rehabilitation Technology has seven cameras outfitted with IR optical filters and an array of IR LEDs, and a set of reflective markers. In this study, the Vicon system was used for trunk sway validation and L5 trace comparison with the K1 and K2.

## NeuroCom System

NeuroCom, a division of Natus is considered as the gold standard balance assessment tool. This is a force plate-based computerized tool for the PT assessment clients with balance and mobility disorders [34]. The NeuroCom follows the disablement model outlined by the World Health Organization (WHO) and provides specific activity results based on a set of defined assessment protocols [47, 48].

The four important NeuroCom protocols used for assessing balance and mobility disorders are,

- Sensory Impairment Assessments
- Motor Impairment Assessments

- Vestibular Ocular Reflex (VOR) Impairment Assessment
- Functional Limitation Assessments

In this study, we considered Unilateral Stance (US) and Tandem Walk (TW), two of the Functional limitation tests for the Kinect sensor validation. Fig. 5 shows a subject performing a US on a NeuroCom System.



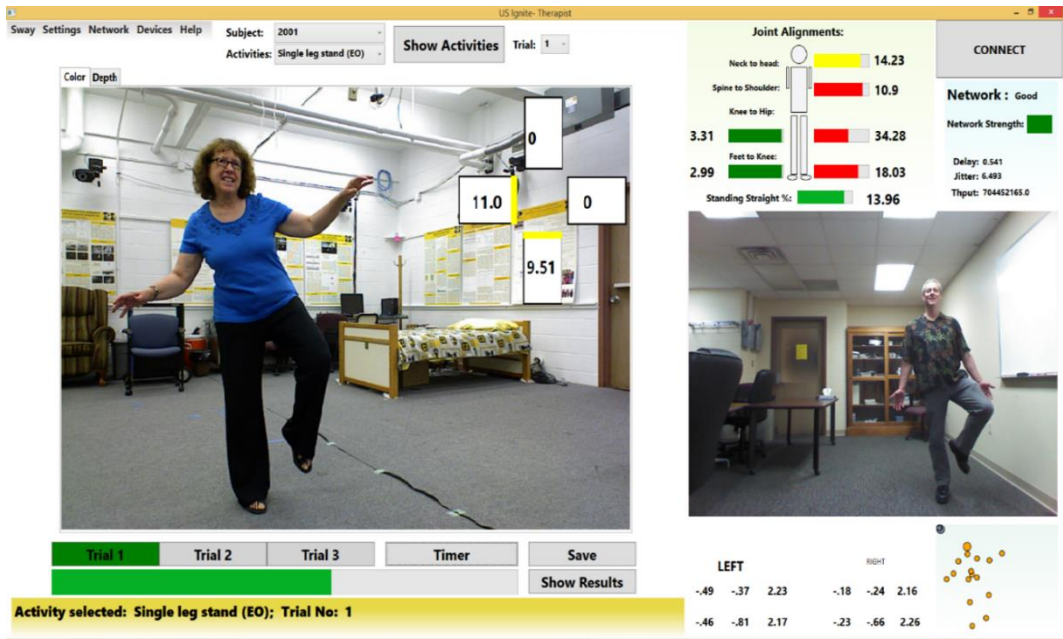
*Figure 5 A subject performing US on a NeuroCom System; taken from [34].*

### Interactive Interfaces for Remote PT

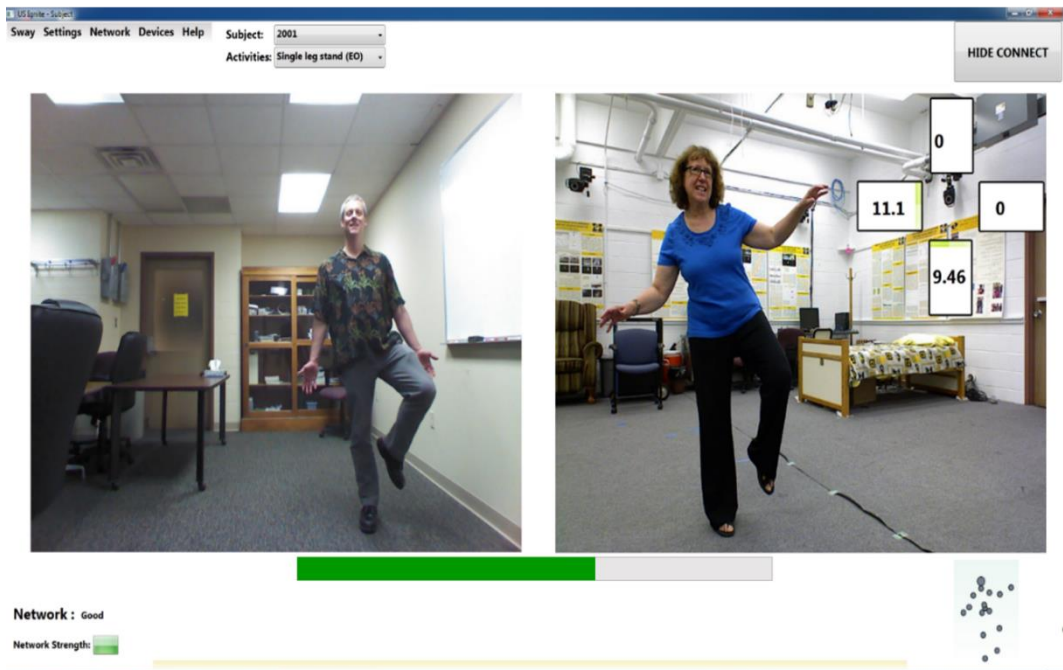
The IPTS consists of two interactive interfaces, one for the PT client in the home and another for the therapist in the clinic. The application interfaces were developed with iterative feedback provided by a therapist with an active clinical practice. Fig. 6 (a) shows the therapist's interface window, which provides real-time visual feedback of kinematic information, measured from the Kinect skeletal data. This includes the AP and ML trunk sway, full body joint alignments, a real-time view of the client's skeletal model, and the status of the network. Dropdown menus and buttons are included to select the subject ID, to select a PT activity, and to select one of the three trials for each PT activity. Every

selection provides a visual feedback by providing information about the selected activity and trial at the bottom of the interface window, and by changing color of the selected trial. Each activity trial is timed for 20 seconds. Finally, a result window displays the post-activity assessment results for all the activities and trials, including a top-down view of the horizontal L5 motion and the maximum AP and ML trunk-sway. Fig. 8 and 9 show the horizontal L5 traces generated for different trials of SLS and TW tests. The result window also displays the actual task performance time in the case of SLS tests, out of the 20 second trial period. Moreover, the therapist's interface supports a set of voice commands to interact with the application, improving user experience.

The interface window for the PT client in the home, displayed in Fig. 6 (b) has a relatively simple interface to help her focus on the activity without distraction. The client interface window includes a timer bar that indicates the time left to perform a particular PT activity and live trunk sway feedback that helps the client to maintain a better form as she performs the activities. These unique features of the IPTS combined with a basic video and audio communication, makes it more than just a video conference system.



(a)



(b)

Figure 6 (a): Therapist's application (b): PT client's application

A modified version of [49] is used to establish a peer to peer communication between the two end users, using RGB, depth, skeletal, and audio data streams received from the Kinect SDK. The application allows to stream these data via sockets. Both the applications behave as server, as well as client. On the server part, there are four listeners to handle managing the underlying socket connection, while also sending the four types of data through:

- ColorListener
- DepthListener
- SkeletonListener
- AudioListener

The application provides a flexibility to choose the type of data stream required. The client and server can use any set of ports to work with data communication. ColorListener takes a parameter in its constructor to determine what type of data should be sent to the client: JPEG (with loss) or PNG (lossless) images or the raw image data. The local and received Kinect data are processed and displayed on the interfaces as per the user requirements and available features. On the client side, there are four clients to connect to the four listeners. To establish a connection, the IP addresses of both network connections should be known. The applications have a special Connect menu to control data communication. Each type of data can be accessed through its specific toggle button. The Kinect sensors can be accessed through one program at a time, using the SDK so to visualize local data, local IP and ports were used to access each type of local data. A public database was used to save IP address data to establish the peer to peer communication. In Fig. 7, shows a block diagram of the IPTS. The unit to process the Kinect sensor data

processes 30 frames per second, making necessary changes on the interface. The Microsoft Kinect studio application was used to save raw data for future analysis and algorithm improvement. The therapist's application accepts voice commands as a key interactive feature, to reduce the use of Mouse or Keyboard. The code word used for each and every command was "MizzouSteps." Before every command, the therapist has to say "MizzouSteps," in order to make the voice recognizer understand a possible command later the word. Some examples voice commands are:

- To show the activity list: "MizzouSteps" + "show activities"
- To select an activity: "MizzouSteps" + "select <NUMBER>"
- To start the timer: "MizzouSteps" + "start timer"

The commands were easy and intuitive, but predefined. Microsoft's System.Speech assembly was used to recognize the voice commands. The *SpeechRecognizer* class provides access to the shared speech recognition service available on the windows desktop[50].

For each PT activity the Kinect depth data and the post-activity results are saved in a local database. These data can be visualized using the same PT interfaces. Fig. 8 and 9 shows two sample result windows for SLS and TW. In Fig. 8, three different horizontal CoM traces along with the max trunk sway in AP (front and back) and ML (left and right) are shown, including the actual performance time. Similarly, in Fig. 9, the tandem walk CoM traces are generated along with the max AP and ML trunk sway values. These values can be overwritten or erased as per requirement.

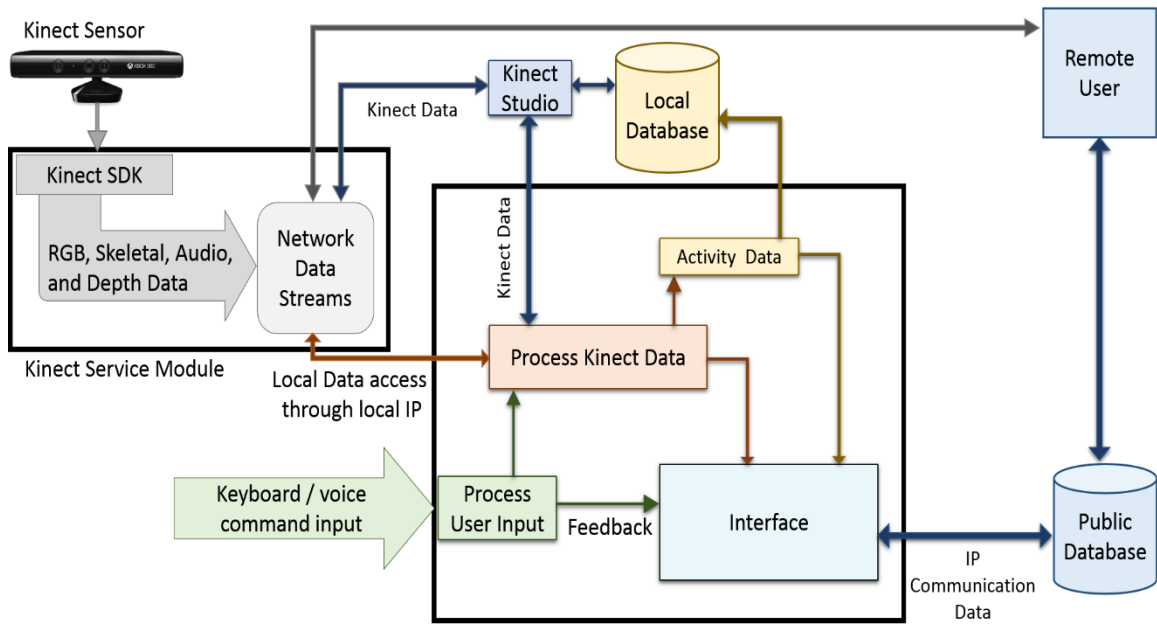


Figure 7 Block Diagram of IPTS.



Figure 8 Result window showing SLS post-activity data.

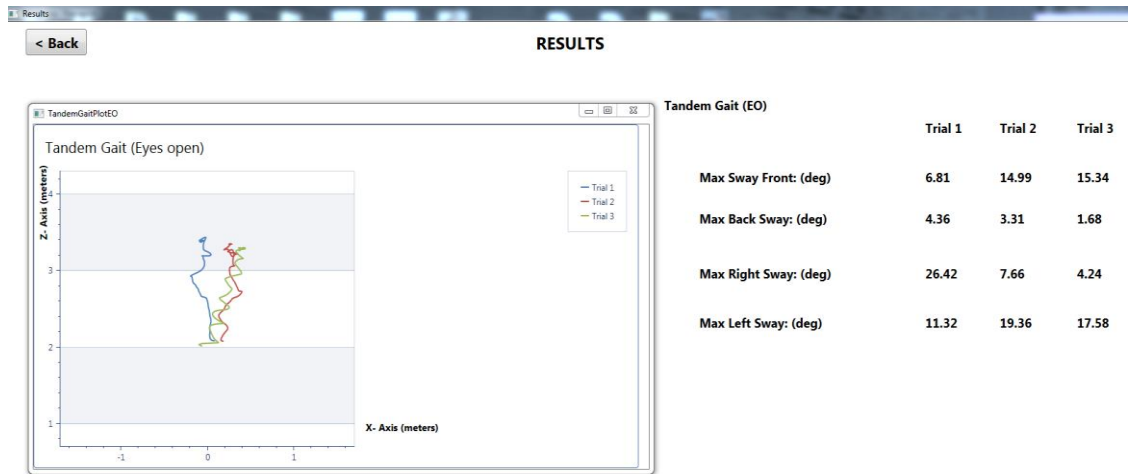


Figure 9 Result window showing TW post-activity data.

## Challenges

The Kinect sensor is not detected as a video conferencing device when connected to a Windows Operating System-based computer. He tried different methods to build a Kinect-based video conferencing system on top of existing video conferencing systems, such as, Skype and Lync. Though we were able to configure Lync to use the Kinect sensor for video and audio communication, we were not able to send depth and skeletal data over the network because of limited features of Lync to work with. This motivated us to make our own video conferencing system using the Kinect. We used the existing Kinect Service code [49] and modified it as per our requirement. We added the voice feedback cancelation module to reduce feedbacks to a reasonable level. Also, we implemented the audio client for the system and upgraded the code to provide Kinect SDK 1.8 compatibility.

The other challenge was providing a suitable network for the data communication. We communicate with a huge amount of Kinect data over network (about 300 Mbps), which requires a high speed low latency network. We requested for a Research-LAN

connection at the University of Missouri, Columbia that provides a 1 Gig network connection and used google fiber at the other test end in Kansas City, MO to achieve our network requirements.

Another challenge was to get the validation data correctly. We had to reject the validation data of eight subjects because of issues in positioning the Kinects and K1's skeletal tracking issues. In the trunk sway validation tests, the Kinects were supposed to be positioned exactly aligning the AP and ML axes as shown in the Fig. 18. In the first set of data collection, we found a larger deviation in the K2's results because of its wrong positioning and orientation.

The Kinect data were saved to local computers using Microsoft Kinect Studio software. After the first data collection with the NeuroCom, when the K1 data was played back using Kinect studio 1.8, the SDK 1.8 was not able to fit the skeletal model on the subjects correctly because of lack of significant body movements in the recordings. In the later data collections, we requested the subjects to walk 3 meters in front of the K1, in order to get the skeletal data correctly from each recording, before each trial. K2 never had a similar issue.

Also, K2 had a higher range of activity recognition as compared to K1 so careful observations were done to position the Kinects and the subject before each data collection.

## Chapter 4

### Methodology

This chapter describes the biomechanical features measured by IPTS and comparison methodologies used to validate it.

#### Biomechanical Features

##### Trunk Sway

The 3D joint location data provided by the Kinect were used to calculate the joint alignments and trunk sway measures. Fig. 10 illustrates the AP and ML trunk sway measures, on its right side. The AP and ML trunk sways are calculated by calculating the angle made by the shoulder center joint with respect to the vertical Y axis at the hip center joint location in AP and ML directions respectively. The trunk sway measures can be calculated as,

$$\theta_{AP} = \tan^{-1} \left( \frac{|(Z_{HiC} - Z_{ShC})|}{|(Y_{HiC} - Y_{ShC})|} \right) \quad (4.1)$$

$$\theta_{ML} = \tan^{-1} \left( \frac{|(X_{HiC} - X_{ShC})|}{|(Y_{HiC} - Y_{ShC})|} \right) \quad (4.2)$$

Where  $\theta_{AP}$  and  $\theta_{ML}$  are the AP and ML trunk sway, and  $(X_{HiC}, Y_{HiC}, Z_{HiC})$  and  $(X_{ShC}, Y_{ShC}, Z_{ShC})$  are the 3D joint locations for hip center and shoulder center respectively.

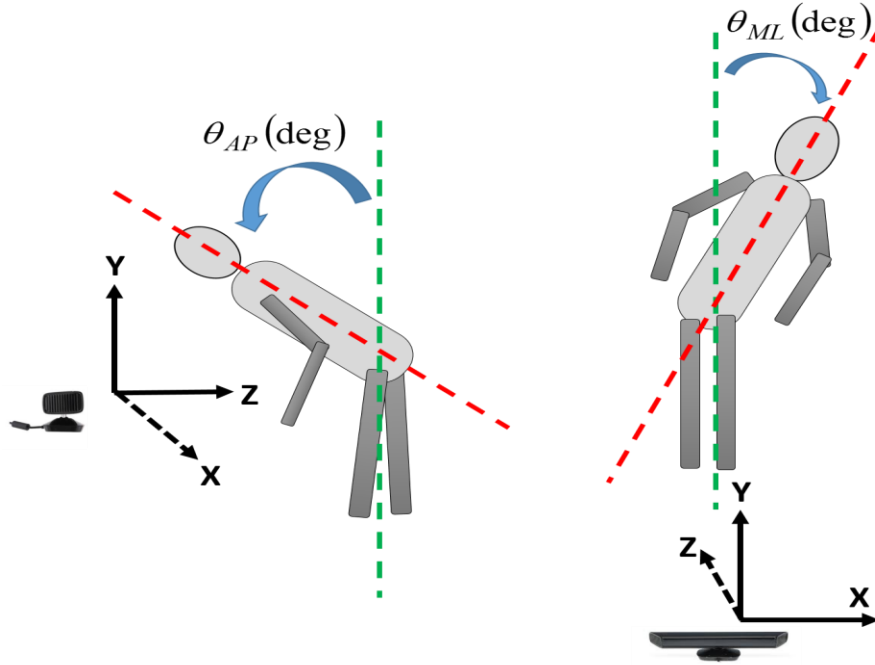


Figure 10 (left): Trunk Sway in AP direction; (right) Trunk Sway in ML direction

Average trunk sway in AP and ML direction is calculated as,

$$\theta_{APavg} = \frac{\sum_{f=1}^{TF} \theta_{APf}}{TF} \quad (4.1.1)$$

$$\theta_{MLavg} = \frac{\sum_{f=1}^{TF} \theta_{MLf}}{TF} \quad (4.2.1)$$

Where,  $\theta_{APavg}$  and  $\theta_{MLavg}$  are the average AP and ML trunk sway and  $TF$  is the total number of frames considered for a particular trial.

Similarly, max AP and ML sway are calculated as,

$$\theta_{APmax} = \max(\{\theta_{APi} : i = 1, \dots, TF\}) \quad (4.1.2)$$

$$\theta_{ML_{\max}} = \max(\{\theta_{MLi} : i = 1, \dots, TF\}) \quad (4.1.2)$$

Where  $\theta_{AP_{\max}}$  and  $\theta_{ML_{\max}}$  are the max trunk sways in AP and ML direction respectively, for a given trial.

### Joint Alignments

The four joint alignments measured were head to neck, shoulder center to spine, hip to knee (left and right), and knee to foot (left and right). For any given frame, the joint alignment was calculated as the angle made by one joint with respect to the vertical axis of the other. The joint alignment can be expressed as,

$$\theta_{JA} = \tan^{-1} \left( \frac{\sqrt{(Z_2 - Z_1)^2 + (X_2 - X_1)^2}}{|(Y_2 - Y_1)|} \right) \quad (4.3)$$

Where  $\theta_{JA}$  represents the joint alignment,  $(X_1, Y_1, Z_1)$  and  $(X_2, Y_2, Z_2)$  are the 3D coordinates of the two joints.

### Single Leg Stance Time Period

For each SLS tests, the actual performance time was measured using the joint alignment measures of knee to hip ( $\theta_{HK}$ ) and ankle to knee ( $\theta_{KA}$ ). Any given depth frame is considered as an actual SLS performed frame, if it satisfies any of the two conditions provide in (4.4) and (4.5).

$$\theta_{KA} \geq \theta_{KA_{\min}} \quad (4.4)$$

$$\theta_{HK} \geq \theta_{HK_{\min}}, \forall \theta_{KA} < \theta_{KA_{\min}} \quad (4.5)$$

Where  $\theta_{HK_{\min}}$  and  $\theta_{KA_{\min}}$  are the minimum threshold values of  $\theta_{HK}$  and  $\theta_{KA}$  respectively.

In this study, we considered  $\theta_{KA_{\min}} = 7$  degree and  $\theta_{HK_{\min}} = 10$  degree for best results.

## Full Body Center of Mass (CoM)

The body center of mass is the mean location of distribution of all body segment masses in space. Full body CoM is calculated using the GEBOD III volume regression equations [51]. The volume regression equations consider two different 17 segment body models for male and female, to measure individual segment volumes of human body. Fig. 11 shows the 17 body segment model for the GEBOD III regression equations.

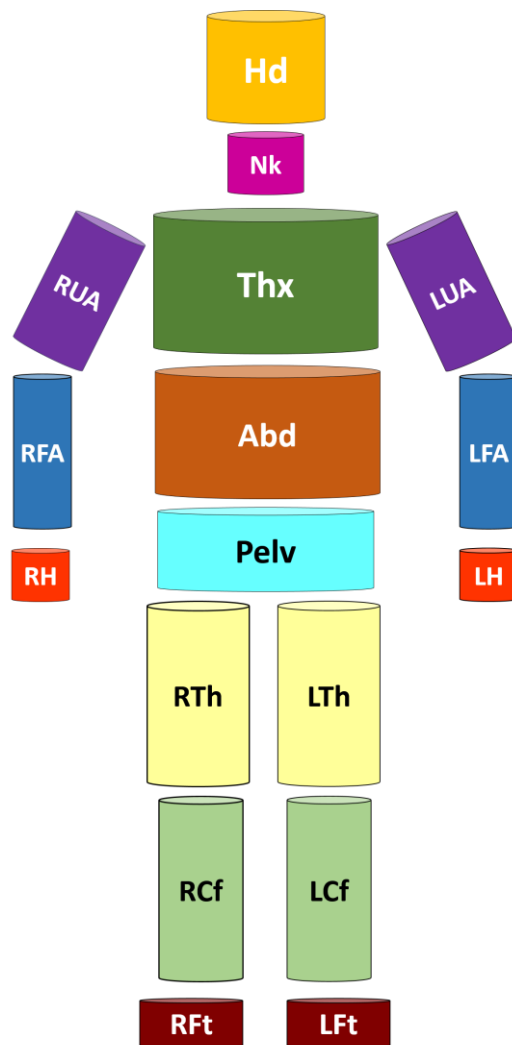


Figure 11 Body Segments for GEBOD III regression equations [51].

This method is based on the 15 segment CoM measurement method by Yang et al. in [52]. They used a Chinese anthropometric data for their study [53].

In Fig. 11, the 17 body segments are:

- **Hd:** Head
- **Nk:** Neck
- **Thx:** Thorax
- **Abd:** Abdomen
- **Pelv:** Pelvis
- **RUA** and **LUA:** Right Upper Arm and Left Upper Arm respectively
- **RFA** and **LFA:** Right Forearm and Left Forearm respectively
- **RH** and **LH:** Right and Left Hand respectively
- **RTh** and **LTh:** Right and Left Thigh respectively
- **RCf** and **LCf:** Right and Left Calf respectively
- **RFt** and **LFt:** Right and Left Foot respectively

The volume regression equations were considered for the adult human male and the adult human female. The regression equations are based on human anthropometric volume data [54, 55]. The predicting variables are weight (lb.) and standing height (in). The predicted segment volumes are in cubic inches. For the volume of each segment, a separate regression equation is given, against the predicting variables. The regression equations are multiple regression equations based on both predicting variables. These equations are based on 46 female subjects and 31 male subjects.

The regression equations for adult female segment volume are:

$$\text{Pelv} = 7.26 * \text{weight} - 15.13 * \text{height} + 555.63 \quad (4.6)$$

$$\text{Abd} = 2.002 * \text{weight} - 17.63 * \text{height} + 1008.7 \quad (4.7)$$

$$\text{Thx} = 7.34 * \text{weight} - 0.19 * \text{height} + 86.47 \quad (4.8)$$

$$\text{Nk} = 0.073 * \text{weight} + 1.55 * \text{height} - 63.89 \quad (4.9)$$

$$\text{Hd} = 0.27 * \text{weight} - 0.19 * \text{height} + 211.61 \quad (4.10)$$

$$\text{RTh} = 3.98 * \text{weight} + 9 * \text{height} - 519.57 \quad (4.11)$$

$$\text{LTh} = 3.98 * \text{weight} + 9 * \text{height} - 519.57 \quad (4.12)$$

$$\text{RCf} = 1.13 * \text{weight} + 1.54 * \text{height} - 65.67 \quad (4.13)$$

$$\text{LCf} = 1.13 * \text{weight} + 1.54 * \text{height} - 65.67 \quad (4.14)$$

$$\text{RFt} = 0.09 * \text{weight} + 1.37 * \text{height} - 58.69 \quad (4.15)$$

$$\text{LFt} = 0.09 * \text{weight} + 1.37 * \text{height} - 58.69 \quad (4.16)$$

$$\text{RUA} = 0.76 * \text{weight} + 0.26 * \text{height} - 28.91 \quad (4.17)$$

$$\text{LUA} = 0.76 * \text{weight} + 0.26 * \text{height} - 28.91 \quad (4.18)$$

$$\text{RFA} = 0.36 * \text{weight} + 0.08 * \text{height} - 0.19 \quad (4.19)$$

$$\text{LFA} = 0.36 * \text{weight} + 0.08 * \text{height} - 0.19 \quad (4.20)$$

$$\text{RH} = 0.06 * \text{weight} + 0.22 * \text{height} - 1.11 \quad (4.21)$$

$$\text{LH} = 0.06 * \text{weight} + 0.22 * \text{height} - 1.11 \quad (4.22)$$

The regression equations for adult male segment volume are:

$$\text{Pelv} = 6.03 * (\text{weight}) - 10.69 * \text{height} + 413.00 \quad (4.23)$$

$$\text{Abd} = 1.18 * \text{weight} - 3.56 * \text{height} + 190.109 \quad (4.24)$$

$$\text{Thx} = 9.98 * \text{weight} - 3.47 * \text{height} + 30.16 \quad (4.25)$$

$$\text{Nk} = 0.38 * \text{weight} - 0.85 * \text{height} + 57.40 \quad (4.26)$$

$$\text{Hd} = 0.12 * \text{weight} + 1.05 * \text{height} + 171.39 \quad (4.27)$$

$$\text{RTh} = 2.79 * \text{weight} + 4.77 * \text{height} - 214.33 \quad (4.28)$$

$$\text{LTh} = 2.79 * \text{weight} + 4.77 * \text{height} - 214.33 \quad (4.29)$$

$$\text{RCf} = 0.72 * \text{weight} + 4.42 * \text{height} - 198.27 \quad (4.30)$$

$$\text{LCf} = 0.72 * \text{weight} + 4.42 * \text{height} - 198.27 \quad (4.31)$$

$$\text{RFt} = 0.12 * \text{weight} + 1.36 * \text{height} - 58.58 \quad (4.32)$$

$$\text{LFt} = 0.12 * \text{weight} + 1.36 * \text{height} - 58.58 \quad (4.33)$$

$$\text{RUA} = 0.85 * \text{weight} - 0.78 * \text{height} + 28.28 \quad (4.34)$$

$$\text{LUA} = 0.85 * \text{weight} - 0.78 * \text{height} - 28.28 \quad (4.35)$$

$$\text{RFA} = 0.47 * \text{weight} - 0.23 * \text{height} + 17.84 \quad (4.36)$$

$$\text{LFA} = 0.47 * \text{weight} - 0.23 * \text{height} + 17.84 \quad (4.37)$$

$$\text{RH} = 0.08 * \text{weight} + 0.29 * \text{height} - 4.42 \quad (4.38)$$

$$\text{LH} = 0.08 * \text{weight} + 0.29 * \text{height} - 4.42 \quad (4.39)$$

The total volume (TV) of the body is calculated as the sum of all the segment volumes calculated above, i.e.

$$TV = \text{Pelv} + \text{Abd} + \text{Thx} + \text{Nk} + \text{Hd} + \text{RTh} + \text{LTh} + \text{RCf} + \text{LCf} + \text{RFt} + \text{RUA} + \text{LUA} \\ + \text{RFA} + \text{LFA} + \text{RH} + \text{LH} \quad (4.40)$$

Now body density can be calculated as,

$$\text{Body Density (D)} = \text{weight}/TV \quad (4.41)$$

And, assuming the body density as constant through the body, individual segment masses can be calculated using the formula,

$$\text{Segment Mass} = \text{Segment Volume} * D \quad (4.42)$$

Equation (4.42) is used to calculate the individual masses of each segment. The center of mass of the human body is calculated as the weighted average of the segment masses with respect to their 3D location. The segment centers were carefully chosen from the Kinect skeletal models for the best fit. Table 1 and 2 presents the 3D points selected to represent the segment centers from the K1 and K2 skeletal model respectively.

*Table 1 SEGMENT CENTERS FOR K1*

<b>Body Segment</b>	<b>K1 body segment center (3D points)</b>
Head	head
Neck	Mid-point between head and shoulder center
Thorax	Mid-point between shoulder center and spine

Abdomen	spine
Pelvis	hip center
Upper arm	Mid-point between shoulder and elbow
Forearm	Mid-point between elbow and wrist
Hand	hand
Thigh	Mid-point between hip and knee
Calf	Mid-point between knee and ankle
Foot	foot

*Table 2 SEGMENT CENTERS FOR K2*

<b>Body Segment</b>	<b>K2 body segment center (3D points)</b>
Head	Head
Neck	neck
Thorax	Mid-point between spine shoulder and spine middle
Abdomen	Mid-point between spine mid and spine base

Pelvis	spine base
Upper arm	Mid-point between shoulder and elbow
Forearm	Mid-point between elbow and wrist
Hand	Mid-point between wrist and hand tip
Thigh	Mid-point between hip and knee
Calf	Mid-point between knee and ankle
Foot	foot

The Kinect joint locations are used to determine the real-time center of mass of a person. The 3D CoM position of the full body is calculated as,

$$comX = \frac{\sum_{i=1}^{17} segmentMass_i \times segmentCenterX_i}{\sum_{j=1}^{17} segmentMass_j} \quad (4.43)$$

$$comY = \frac{\sum_{i=1}^{17} segmentMass_i \times segmentCenterY_i}{\sum_{j=1}^{17} segmentMass_j} \quad (4.44)$$

$$comZ = \frac{\sum_{i=1}^{17} segmentMass_i \times segmentCenterZ_i}{\sum_{j=1}^{17} segmentMass_j} \quad (4.45)$$

Where comX, comY, and comZ are the 3D coordinates center of mass of the human body and ‘i’ represents each segment.

#### CoG and CoM plots

“The CoM of body segment mass distribution in space is the point where the weighted relative position of the distribution mass sums to zero. CoG is the point in a body around which the resultant torque due to gravity forces vanishes. A place where a gravity field can be considered to be uniform, the CoM and the CoG will be the same” [56](web page). Therefore, in this study we can consider the CoM and CoG points to be same assuming uniform gravity field in a lab environment.

CoG and CoM plots are the horizontal traces of the motion of Center of Gravity and Center of Mass of a person. Force-plate-based NeuroCom system provides a CoG plot, whereas, the Kinect-based IPTS provides a CoM plot at the end of each trial. The CoG and CoM plots provide a top-down view of postural sway. Fig. 12 and Fig. 13 provide a comparison of CoG and CoM-based plots for the same set of single leg stance and tandem walk trials from NeuroCom, and the two Kinects, respectively.

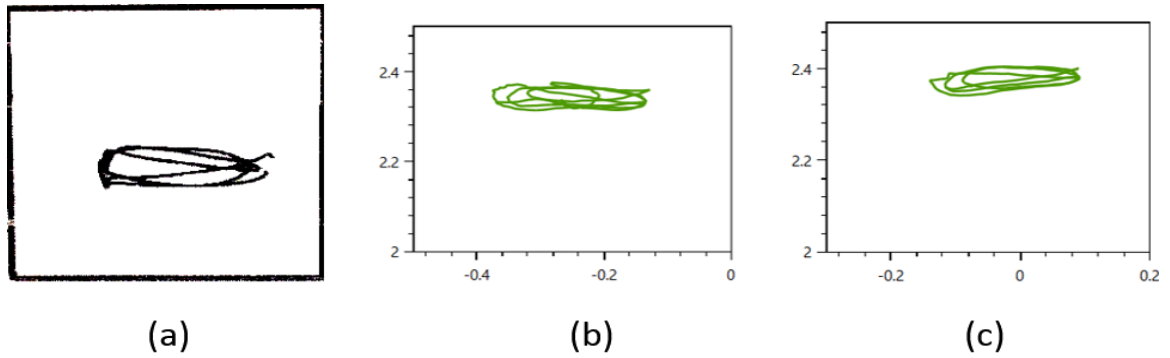


Figure 12 Single leg stance plots: (a): CoG plot from NeuroCom; (b) CoM plot from K1; (c): CoM plot from K2.

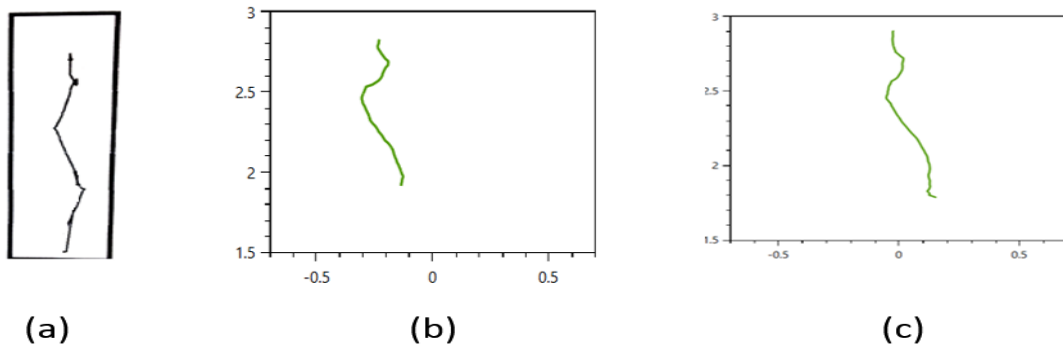


Figure 13 Tandem walk plots: (a): CoG plot from NeuroCom; (b) CoM plot from the K1; (c): CoM plot from the K2.

The plots provide a visual feedback of postural sway and deviation from normal gait and posture. This is a very important information for physical therapists for postural balance estimation.

#### Postural Sway Angle (deg)

The postural sway angle is measured as the vertical angle between center of mass and between ankles. In Fig. 14,  $\theta_s$  represents the postural sway angle.

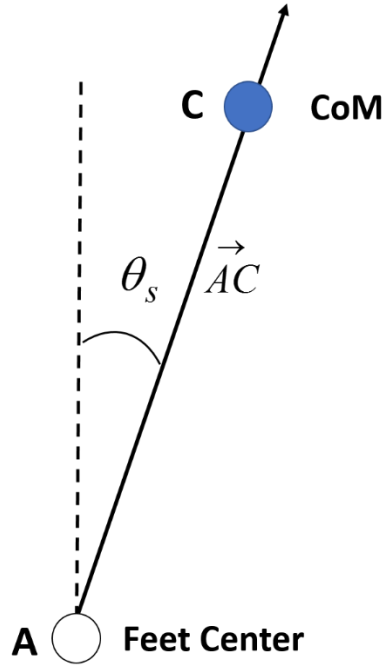


Figure 14 Sway Angle Representation.

Sway angle is measured as,

$$\theta_s = \tan^{-1} \left( \frac{\sqrt{(comZ - Z_{ft})^2 + (comX - X_{ft})^2}}{|comY - Y_{ft}|} \right) \quad (4.46)$$

Where  $X_{ft}$ ,  $Y_{ft}$  and  $Z_{ft}$  represent the 3D coordinates of the feet center or the middle point between the two ankles and are measured as,

$$X_{ft} = \frac{X_{ftR} + X_{ftL}}{2} \quad (4.47)$$

$$Y_{ft} = \frac{Y_{ftR} + Y_{ftL}}{2} \quad (4.48)$$

$$Z_{ft} = \frac{Z_{ftR} + Z_{ftL}}{2} \quad (4.49)$$

Where  $x_{ftR}, y_{ftR}, z_{ftR}$  &  $x_{ftL}, y_{ftL}, z_{ftL}$  are the X, Y, and Z coordinates of right and left foot respectively.  $\vec{AC}$  is considered as the sway vector.

Sway velocity (deg/sec)

Sway velocity is determined by measuring the change in postural sway per unit time. Sway velocity can be calculated as the sum of total angle change of sway vector over unit time period. In Fig. 15,  $\theta_{Ch}$  represents the vector angle between the sway vectors,  $\vec{AC1}$  and  $\vec{AC2}$ .

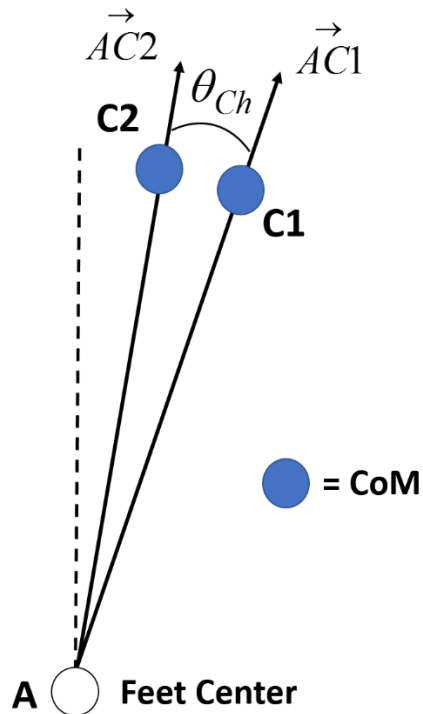


Figure 15 Sway vector angle representation ( $\theta_{Ch}$ ).

Sway velocity per T seconds is calculated as,

$$V_{sway} = \frac{\sum_{i=1}^T \theta_{Ch}}{T} \quad (4.50)$$

and

$$\theta_{Ch} = \cos^{-1} \left( \frac{((C1X - X_{ft}) * (C2X - X_{ft})) + ((C1Y - Y_{ft}) * (C2Y - Y_{ft})) + ((C1Z - Z_{ft}) * (C2Z - Z_{ft}))}{\sqrt{((C1X - X_{ft})^2 + (C1Y - Y_{ft})^2 + (C1Z - Z_{ft})^2)} \sqrt{((C2X - X_{ft})^2 + (C2Y - Y_{ft})^2 + (C2Z - Z_{ft})^2)}} \right) \quad (4.51)$$

Where,  $i$  represents unit time and (C1X, C1Y, C1Z) and (C2X, C2Y, C2Z) are the coordinates of C1 and C2 points.

Step width (cm)

Step width is the average lateral separation between the left and right foot, while performing a tandem walk. Fig. 16, represents the step width  $W$ , while performing a tandem walk.

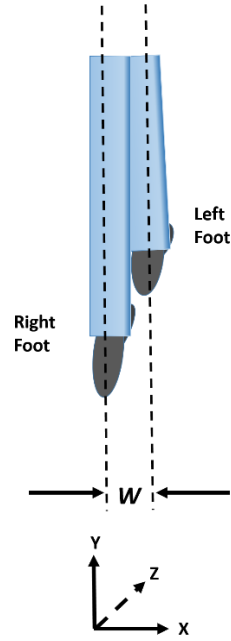


Figure 16 (Front view of Tandem Walk) Step width representation ( $W$ ).

$W$  is measured as the average absolute difference in  $X$  coordinate values between the right and left foot.

$$W = \frac{\sum_{i=1}^T (|RfX_i - LfX_i|)}{T} \quad (4.52)$$

Where,  $RfX_i$  and  $LfX_i$  are the  $X$  coordinates of right and left foot for each frame  $i$  and  $T$  is the total time period.

Speed (cm/sec)

Speed ( $u$ ) is measured as the distance covered by the CoM per unit time and can be represented as,

$$u = \frac{\sum_{i=1}^{T-1} (comZ(i) - comZ(i+1))}{T} \quad (4.53)$$

Where  $T$  is the total time period and  $(comX(i), comY(i), comZ(i))$ ,  $(comX(i+1), comY(i+1), comZ(i+1))$  are the 3D coordinates of center of mass at time  $i$  and  $i+1$ .

End Sway (deg/sec)

End sway is the sway velocity of the CoG sway in the anterior-posterior direction for 5 seconds beginning when the PT client terminates walking.

AP and ML Sway Range (cm)

These are the maximum sways in AP and ML direction, while performing a SLS test. Fig. 17 shows the AP and ML sway range for a SLS test.

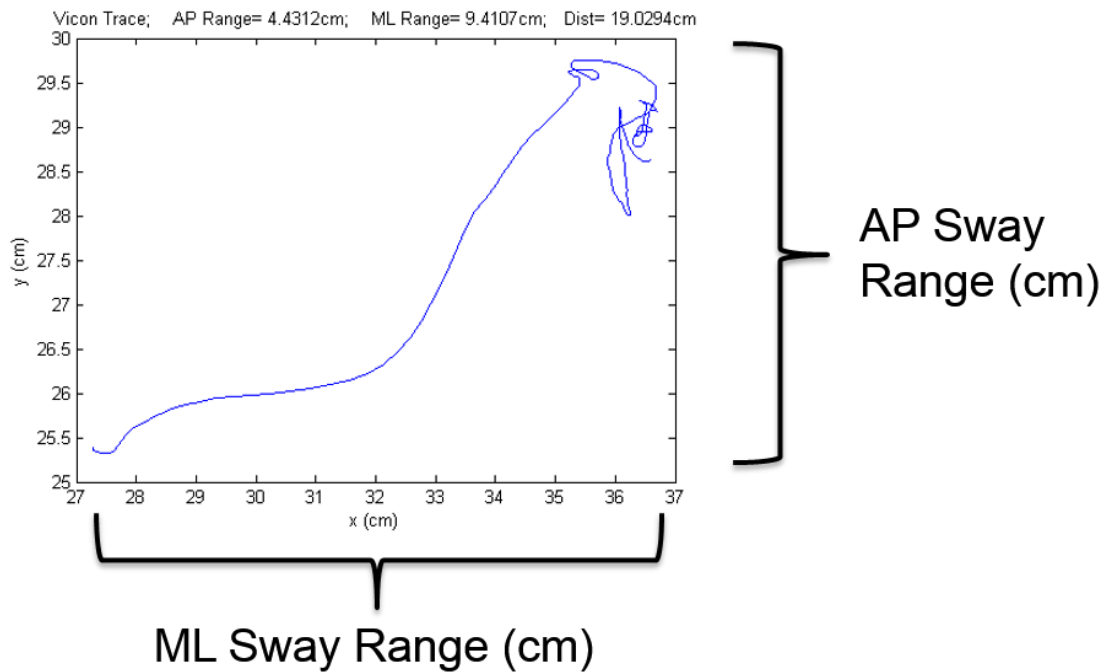


Figure 17 AP and ML Sway Range

## Validation Methods

### Validation with the Vicon System

A Vicon motion capture system was used to validate the biomechanical features measured using the skeletal data from the Kinect SDKs as described in section II. The two Kinect SDKs produce different sets of 3D skeletal joint positions. The 3D skeletal position data from the sternum (SDK 1.8: shoulder center and SDK 2.0: spine shoulder) and hip center (SDK 1.8: hip center and SDK 2.0: spine base) were used to calculate the trunk sway. The data collection for Kinect K1 was done using the Windows 7 operating system (OS), whereas the Windows 8.1 OS was used to collect the data for Kinect K2. Windows 7 was used for K1 due to substantial frame drops in Windows 8.1. For the Vicon system, markers were attached to the subjects' mid-sternum, L5, C7, anterior superior iliac spines (RASI and LASI), and posterior superior iliac spines (RPSI and LPSI) and their 3D positions were recorded in synchronization with the Kinects. Four subjects participated in this validation test. The subjects were asked to perform 3 trials for each of the tests: single leg stance with eyes open (SLS EO), single leg stance with eyes closed (SLS EC), tandem walk with eyes open (TW EO), and tandem walk with eyes closed (TW EC). The tandem walk task was defined as a five step heel to toe walk.

Fig. 18 shows the placement of the human subject in the global coordinate systems of the Vicon, K1, and K2 during the data collection. The correct alignment of the person with respect to the global coordinates of the K1, K2, and the Vicon is highly necessary to get correct results. K1 and K2 were placed with a distance of <1 cm apart during the tests and were properly aligned with the AP and ML axes.

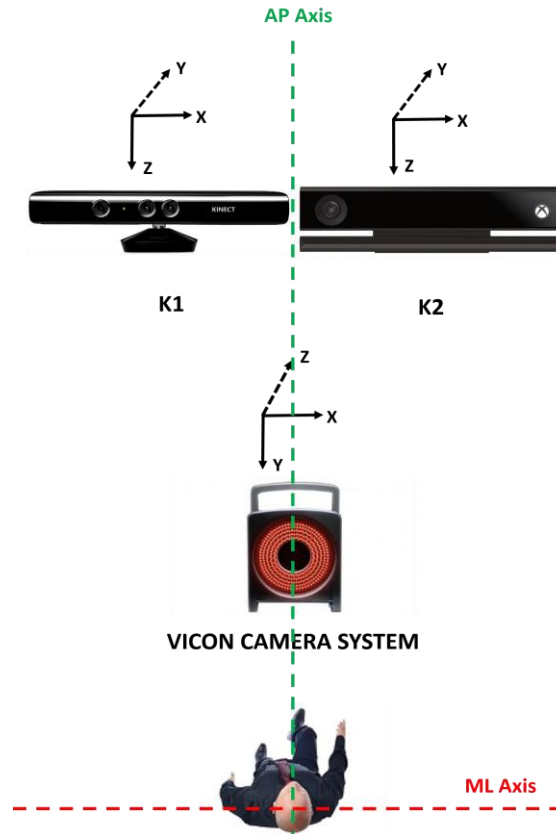


Figure 18 AP and ML trunk sway axis with respect to global coordinates of K1, K2, and Vicon.

#### Validation of Full-Body CoM measurements

In order to validate the Full-Body CoM measurement method, we did another validation study using the left and right foot SLS data from the Mizzou Motion Analysis Center, University of Missouri, Columbia, MO. Vicon and Force plates were used for the ground truth data. They used only the K2 sensor for data collection, instead of both K1 and K2. The dataset contains data of 7 subjects.

#### Validation with the NeuroCom System

The NeuroCom long force plate system was used to validate the bio-mechanical features of SLS and TW tests. The full body skeletal models from the K1 and K2 were

considered for this test. The 3D location of full body CoM was obtained for the Kinect skeletal models, using the GEBOD volume regression equations [51]. Fig. 19 demonstrates the experimental set up for the data collection of this validation study.

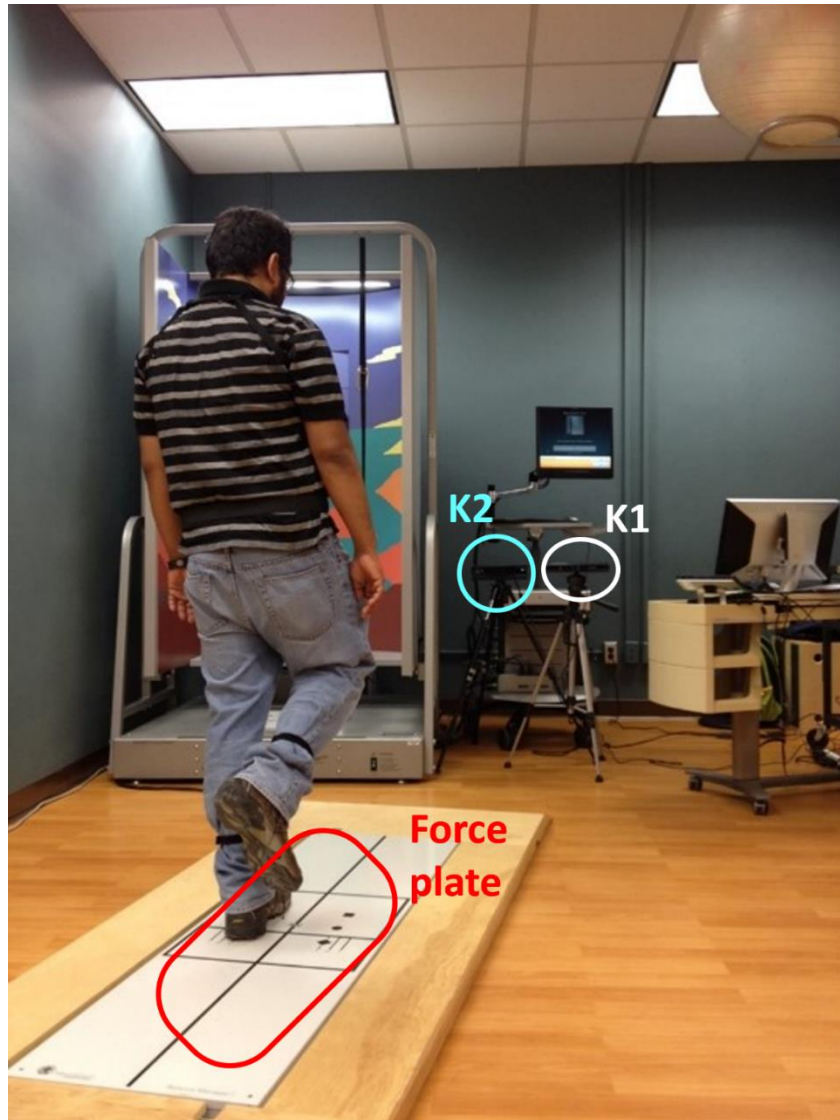


*Figure 19 Subject performing SLS for the NeuroCom, K1, and K2 validation.*

Four subjects participated in this validation test. The subjects were asked to perform three trials for each of the tests: single leg stance with eyes open (SLS EO), single leg stance with eyes closed (SLS EC), tandem walk with eyes open (TW EO), and tandem

walk with eyes closed (TW EC). The US test from NeuroCom was considered for SLS validation. For the tandem walk test validation, the TW test from NeuroCom was considered. A hand wave gesture was used for synchronization of the Kinects with the other systems. Finally, the CoM and joint data from the K1 and K2 were preprocessed with a median filter to remove noise.

The results obtained from NeuroCom for the comparison were the actual results obtained at the end of each test through the Balance Master software. The K1 and K2 data processing were done using the hand movement synchronization and with the best of our observation. The data processing was repeated several times to confirm the results and avoid subjective observation issues. At maximum, a deviation of  $\pm 0.2$  unit can be expected for each result.

## Chapter 5

### Results and Discussion

This chapter contains the Vicon and NeuroCom validation results followed by discussion for each.

#### Trunk Sway Validation with the Vicon System

Tables 3 and 4 show the comparisons between the each Kinect type and the Vicon system. In every test, K2 performed better in calculating AP trunk sway as compared to K1.

*Table 3 TRUNK SWAY ANGLE DEVIATION FOR THE SINGLE LEG STANCE TEST COMPARED TO THE VICON*

<b>Avg. Trunk Sway Deviation (deg)</b>	<b>K1</b>				<b>K2</b>			
	<i>Eyes Open</i> ( $u \pm \sigma$ )	<i>Avg. diff</i> (%)	<i>Eyes Closed</i> ( $u \pm \sigma$ )	<i>Avg. diff</i> (%)	<i>Eyes Open</i> ( $u \pm \sigma$ )	<i>Avg. diff</i> (%)	<i>Eyes Closed</i> ( $u \pm \sigma$ )	<i>Avg. diff</i> (%)
AP	0.3 ± 1.3	47.8	2.0 ± 2.5	83.7	-0.1 ± 0.9	27.2	-0.3 ± 0.8	8.0
ML	1.9 ± 0.7	39.2	3.1 ± 2.2	41.2	2.0 ± 0.7	41.5	2.4 ± 1.5	33.5

Table 4 TRUNK SWAY ANGLE DEVIATION FOR THE TANDEM WALK TEST COMPARED TO THE VICON

Avg. Trunk Sway Deviation (deg)	K1				K2			
	Eyes Open ( $u \pm \sigma$ )	Avg. diff (%)	Eyes Closed ( $u \pm \sigma$ )	Avg. diff (%)	Eyes Open ( $u \pm \sigma$ )	Avg. diff (%)	Eyes Closed ( $u \pm \sigma$ )	Avg. diff (%)
AP	3.4 ± 4.6	47.8	3.4 ± 1.8	57.3	-0.1 ± 4.1	33.0	-0.6 ± 1.1	13.1
ML	1.2 ± 1.2	36.2	1.5 ± 1.4	27.2	1.4 ± 1.0	48.3	1.7 ± 1.0	30.38

In SLS tests, the maximum average AP trunk sway deviation ( $u \pm \sigma$ ) measured by K1 was  $2.0 \pm 2.5$  whereas it was  $-0.3 \pm 0.8$  by K2. Again, the maximum average ML trunk sway deviation measured in SLS tests were  $3.1 \pm 2.2$  and  $2.4 \pm 1.5$  by K1 and K2 respectively. In TW tests, the maximum average trunk sway deviation ( $u \pm \sigma$ ) measured in the AP direction by K1 and K2 were  $3.4 \pm 4.6$  and  $-0.6 \pm 1.1$  respectively. However, the maximum average trunk sway deviation ( $u \pm \sigma$ ) measured in the ML direction by K1 and K2 were  $1.5 \pm 1.4$  and  $1.7 \pm 1.0$ . Results show that the performance of K1 in measuring ML trunk sway was slightly better than K2 in most cases but the results were very close. For performance across all of the trials, the maximum trunk sway deviation measured by K1 in the AP and ML directions were 17.24 degree and 7.29 degree, respectively. The maximum trunk sway deviation measures in the AP and ML directions for K2 were 12.75 degree and 5.63 degree, respectively. Overall, K2 performed slightly better with a more stable skeletal model and larger range for activity tracking as compared to the K1.

#### Full-Body CoM measurement comparison with the Vicon and Forceplate system

For this validation, the data from Mizzou Motion Analysis Center, University of Missouri were used. The body CoM estimated from plugin gait model of Vicon and the

Center of Pressure (CoP) measurements from the Forceplate system were compared with the Full-Body CoM estimation from the Kinect data using our GEBOD regression method as mentioned in Chapter 4. We considered AP and ML Sway Range measures for this validation. Table 5 shows the Sway Range deviation results for AP and ML Sway Range.

Table 5 SWAY RANGE DEVIATION FOR THE SINGLE LEG STANCE TEST COMPARED TO THE VICON AND FORCEPLATE

Sway Range Deviation (cm)	K2-Vicon				K2-Forceplate			
	Right Foot ( $u \pm \sigma$ )	Avg. diff (%)	Left Foot ( $u \pm \sigma$ )	Avg. diff (%)	Right Foot ( $u \pm \sigma$ )	Avg. diff (%)	Left Foot ( $u \pm \sigma$ )	Avg. diff (%)
AP	-1.5 ± 3.5	25.4	0.0 ± 0.4	15.9	-2.9 ± 2.3	41.1	-1.2 ± 0.7	26.5
ML	-1.4 ± 1.2	10.2	-1.0 ± 0.8	9.5	-3.9 ± 1.7	24.1	-4.1 ± 1.4	28.4

The sway range deviation in ML direction was always higher as compared to AP directions. The average % deviation were relatively low for the comparison with Vicon as compared to forceplate. When the Kinect results are compared to the Vicon system, it's a CoM to CoM comparison, whereas the comparison between the Kinect and the Forceplate is a CoM to CoP comparison. This is the reason why we get a higher deviation when compared to the Forceplate as compared to the Vicon.

### Validation with the NeuroCom System

The two Kinects were validated with the NeuroCom System. SLS and TW tests were considered for this validation test. The biomechanical features measured for SLS test were:

- Sway Velocity (deg/sec)
- CoG/CoM Plot

The biomechanical measures considered for TW test were:

- Step Width (cm)
- Speed (cm/sec)
- End Sway (deg/sec)
- CoG/CoM Plot

#### NeuroCom validation Results

Table 6 shows a comparison of deviation measured in calculating Sway Velocity between the each Kinect type and NeuroCom System.

*Table 6 SWAY VELOCITY DEVIATION FOR THE SINGLE LEG STANCE TEST COMPARED TO THE NEUROCOM*

Sway Velocity Deviation (deg/sec)	K1				K2			
	<i>Eyes Open</i> ( $u \pm \sigma$ )	<i>Avg. diff</i> (%)	<i>Eyes Closed</i> ( $u \pm \sigma$ )	<i>Avg. diff</i> (%)	<i>Eyes Open</i> ( $u \pm \sigma$ )	<i>Avg. diff</i> (%)	<i>Eyes Closed</i> ( $u \pm \sigma$ )	<i>Avg. diff</i> (%)
	0.3 ± 0.4	32.0	1.7 ± 2.4	36.6	0.1 ± 0.4	32.6	1.5 ± 1.6	27.6

In both EO and EC tests, K2 performed slightly better as compared to the K1. For performance across all the trials, the maximum sway velocity deviation measured by K1 was 6.9 deg/sec, whereas the maximum sway velocity deviation measured by K2 was 5.1 deg/sec.

Table 7 shows a comparison of deviations measured in calculating Step Width between the each Kinect type and NeuroCom System.

Table 7 STEP WIDTH DEVIATION FOR THE TANDEM WALK TEST COMPARED TO THE NEUROCOM

Step Width Deviation (cm)	K1				K2			
	<i>Eyes Open</i> ( $u \pm \sigma$ )	<i>Avg. diff</i> (%)	<i>Eyes Closed</i> ( $u \pm \sigma$ )	<i>Avg. diff</i> (%)	<i>Eyes Open</i> ( $u \pm \sigma$ )	<i>Avg. diff</i> (%)	<i>Eyes Closed</i> ( $u \pm \sigma$ )	<i>Avg. diff</i> (%)
	2.6 ± 5.4	28.9	8.7 ± 9.1	46.6	4.1 ± 5.2	34.5	8.5 ± 9.0	44.3

In all tests, the step width deviation measures by K1 and K2 were somewhat high. We believe, the increased deviation values are because of the inability of Kinect skeletal models in fitting Foot joints when one foot is not visible to the sensor, resulting noisy 3D coordinates assigned to the hidden foot. Fig. 20 (a) and (b) show the issue in the two skeletal models of K1 and K2. The distortions in K1 were slightly more as compared to K2 but they both performed equally bad in determining the foot joint location, especially when subject performed badly. The deviations were very high for subject three as compared to the rest. Table 8 provides a comparison deviations measured in calculating Step Width between the each Kinect type and NeuroCom System without considering results of Subject 3. We can see a good improvement in the deviation results in Table 8. We assume that the higher deviation results for Subject 3 could be because of his extreme bad performance and the Kinect sensor’s inability to capture skeletal data accurately.

Table 8 STEP WIDTH DEVIATION FOR THE TANDEM WALK TEST COMPARED TO THE NEUROCOM WITH OUT CONSIDERING DEVIATIONS OF SUBJECT 3

Step Width Deviation (cm)	K1				K2			
	<i>Eyes Open</i> ( $u \pm \sigma$ )	<i>Avg. diff</i> (%)	<i>Eyes Closed</i> ( $u \pm \sigma$ )	<i>Avg. diff</i> (%)	<i>Eyes Open</i> ( $u \pm \sigma$ )	<i>Avg. diff</i> (%)	<i>Eyes Closed</i> ( $u \pm \sigma$ )	<i>Avg. diff</i> (%)
	0.0 ± 1.6	17.6	3.8 ± 3.4	34.7	1.1 ± 0.8	20.7	3.6 ± 3.4	32.4

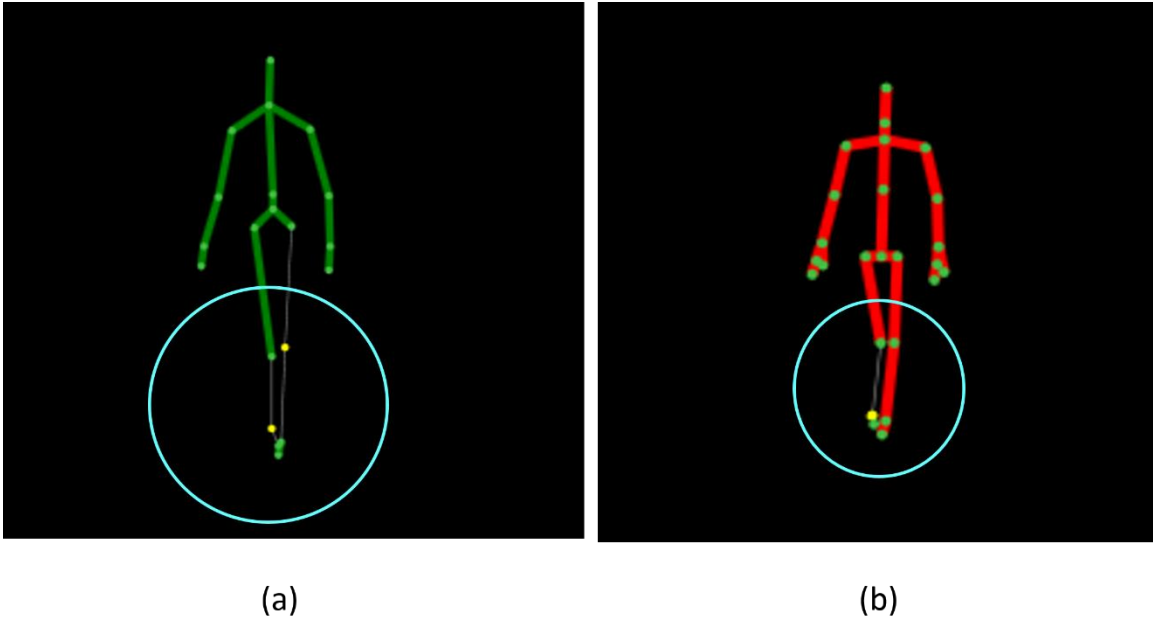


Figure 20 Skeletal model of subject while performing TW by (a): K1; (b): K2 SDKs. The blue ring in each image shows the distorted skeletal joints.

Table 9 shows a comparison of deviations measured in calculating forward walk speed between the each Kinect type and NeuroCom System during TW tests. The speed values were calculated considering the CoM motion in Z direction i.e. towards the Kinects.

Table 9 SPEED DEVIATION FOR THE TANDEM WALK TEST COMPARED TO THE NEUROCOM: Using CoM Method

Speed Deviation (cm/sec)	K1				K2			
	<i>Eyes Open</i> ( $u \pm \sigma$ )	<i>Avg. diff</i> (%)	<i>Eyes Closed</i> ( $u \pm \sigma$ )	<i>Avg. diff</i> (%)	<i>Eyes Open</i> ( $u \pm \sigma$ )	<i>Avg. diff</i> (%)	<i>Eyes Closed</i> ( $u \pm \sigma$ )	<i>Avg. diff</i> (%)
	3.3 ± 3.4	18.2	1.0 ± 2.9	19.8	2.0 ± 1.8	11.5	1.0 ± 2.5	19.7

The K1 and K2 performed almost similar with K2 performing slightly better in determining forward tandem walk speed. The speed deviation measures were close to zero

in EC tests as compared to eyes open tests. In eyes open tests, the subjects usually perform the tasks faster as compared to eyes closed tests. Therefore, we assume that our method would provide better speed measures for an elderly population as compared to a younger population because of the significant difference in their walking speed. For performance across all the trials, the maximum speed deviation measured by the K1 was 8.6 cm/sec, whereas the maximum speed deviation measured by the K2 was 4.9 cm/sec. Extending this experiment, we measured the forward speed of each subject using the Spinal joint instead of the CoM. The results were very similar.

*Table 10 SPEED DEVIATION FOR THE TANDEM WALK TEST COMPARED TO THE NEUROCOM: Using Spinal Joint Alone*

<b>Speed Deviation (cm/sec)</b>	<b>K1</b>				<b>K2</b>			
	<i>Eyes Open</i> ( $u \pm \sigma$ )	<i>Avg. diff</i> (%)	<i>Eyes Closed</i> ( $u \pm \sigma$ )	<i>Avg. diff</i> (%)	<i>Eyes Open</i> ( $u \pm \sigma$ )	<i>Avg. diff</i> (%)	<i>Eyes Closed</i> ( $u \pm \sigma$ )	<i>Avg. diff</i> (%)
	2.8 ± 3.0	16.3	0.3 ± 2.8	20.4	2.0 ± 1.8	10.9	0.9 ± 2.7	20.8

The deviation results in Table 10 show that the results are very close to that of the CoM method results in Table 9. The K1 performed better in determining speed for eyes closed trials. Rest of the results remain almost the same.

Table 11 shows a comparison of deviations measured in calculating End Sway between the each Kinect type and NeuroCom System during TW tests. For this test the evaluation of AP Sway Velocity was conducted when the subjects completed the TW and were 2.1 meter away from the Kinects.

Table 11 END SWAY DEVIATION FOR THE TANDEM WALK TEST COMPARED TO THE NEUROCOM

End Sway Deviation (deg/sec)	K1				K2			
	<i>Eyes Open</i> ( $u \pm \sigma$ )	<i>Avg. diff</i> (%)	<i>Eyes Closed</i> ( $u \pm \sigma$ )	<i>Avg. diff</i> (%)	<i>Eyes Open</i> ( $u \pm \sigma$ )	<i>Avg. diff</i> (%)	<i>Eyes Closed</i> ( $u \pm \sigma$ )	<i>Avg. diff</i> (%)
	1.3 ± 2.0	75.0	4.1 ± 2.9	67.4	1.2 ± 1.4	58.2	3.6 ± 3.1	55.6

Similar to SLS Sway Velocity measures, End Sway measure deviations for both Kinects were more for eyes closed tests as compared to eyes open tests. We assume that in case of TW tests, subjects are more unstable in their AP postural balance and the Kinect sensors does not have a high sensitivity to AP movement variations to capture it. However, K2 performed slightly better with lower deviation rates but we can consider both Kinects performed average in capturing this biomechanical measure.

The CoG and CoM plots from the NeuroCom and Kinects, respectively, were very comparable. The Kinect results have close similarities and details as that of the NeuroCom results. Fig. 21 shows a set of two results for SLS and TW with CoG plots from NeuroCom and CoM plots from Kinects.

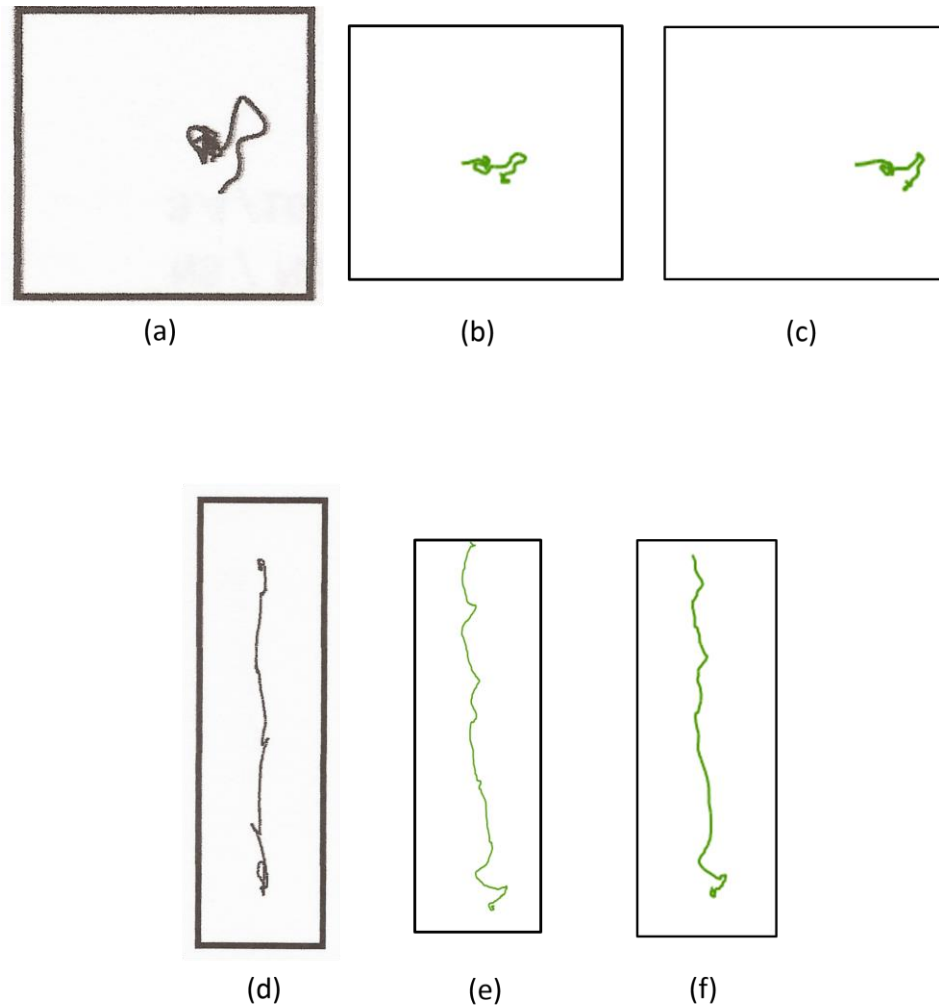


Figure 21 SLS (a): CoG plot by NeuroCom; SLS CoM plot by (b): K1; (c): K2; TW (d): CoG plot by NeuroCom; TW CoM plot by (e): K1; (f): K2.

Detailed sway details were noticed in the CoM traces of Kinects, proving high accuracy of CoM traces. Appendix A has a list of all the CoG, CoM traces computed during this study for all four subjects.

#### The NeuroCom Classification Accuracy

NeuroCom follows a simple data representation method using color codes as discussed in chapter two. The results are classified as bad or good using red or green colors,

respectively. The results from the Kinects were compiled to compare the color code results. Table 12 shows the result classification for each subject for Mean Sway Velocity calculation in SLS tests.

Table 12 CLASSIFICATION OF MEAN COM SWAY VELOCITIES COMPARED TO THE NEUROCOM

Mean Sway Velocity (deg/s)	NeuroCom		K1		K2	
	<i>EO</i>	<i>EC</i>	<i>EO</i>	<i>EC</i>	<i>EO</i>	<i>EC</i>
Subject 1	0.9	2.5	0.62	2.66	0.83	1.88
Subject 2	0.8	3.7	1.02	3.31	0.99	2.95
Subject 3	1.9	10.3	0.98	4.83	1.29	6.63
Subject 4	0.9	2.9	0.68	1.57	0.79	2.05

The Mean Sway Velocity classification accuracy for K1 was 80%, whereas it was 87.5% for K2. Table 13 shows the result classification for each subject for Step Width calculation in TW tests.

Table 13 CLASSIFICATION OF STEP WIDTH COMPARED TO THE NEUROCOM

Mean Step Width (cm)	NeuroCom		K1		K2	
	<i>EO</i>	<i>EC</i>	<i>EO</i>	<i>EC</i>	<i>EO</i>	<i>EC</i>
Subject 1	6.9	8.8	7.3	6.9	6.6	7.3
Subject 2	5.4	9.3	4.5	3.9	4.0	4.0
Subject 3	16.0	28.6	5.4	4.9	5.0	5.6
Subject 4	9.2	12.4	9.5	8.2	7.6	8.1

The Mean Step Width classification accuracy for the K1 and K2 was same i.e. 62.5%. It shows that the K1 and K2 both significantly missed the step width measures because of higher distortion of skeletal model. Table 14 shows the result classification for each subject for forward walk speed calculation in TW tests.

Table 14 CLASSIFICATION OF SPEED COMPARED TO THE NEUROCOM

Mean Speed (cm/sec)	NeuroCom		K1		K2	
	<i>EO</i>	<i>EC</i>	<i>EO</i>	<i>EC</i>	<i>EO</i>	<i>EC</i>
Subject 1	26.2	17.4	19.3	16.4	23.7	15.7
Subject 2	17.5	14.0	17.4	11.5	15.9	12.4
Subject 3	12.2	7.1	10.5	9.4	11.1	9.6
Subject 4	20.3	20.0	15.7	17.2	17.8	16.7

The Mean Step Width classification accuracy for the K1 was 87.5%, whereas it was 100% for K2. Table 15 shows the result classification for each subject for End Sway calculation in TW tests.

Table 15 CLASSIFICATION OF END SWAY COMPARED TO THE NEUROCOM

Mean End Sway (deg/s)	NeuroCom		K1		K2	
	<i>EO</i>	<i>EC</i>	<i>EO</i>	<i>EC</i>	<i>EO</i>	<i>EC</i>
Subject 1	2.9	2.8	0.8	0.7	0.5	1.1
Subject 2	3.0	5.1	4.3	2.9	3.6	4.0
Subject 3	3.4	10.9	0.9	2.5	1.0	2.4
Subject 4	2.56	6.16	0.6	1.2	1.1	2.2

The Mean End Sway classification accuracy for the K1 and K2 were same i.e. 87.5%. The results show both the Kinects missed some important AP sway measures. Fig. 22 shows a bar plot representing classification accuracy for each type of measurement: Sway Velocity, Step Width, Speed, and End Sway.

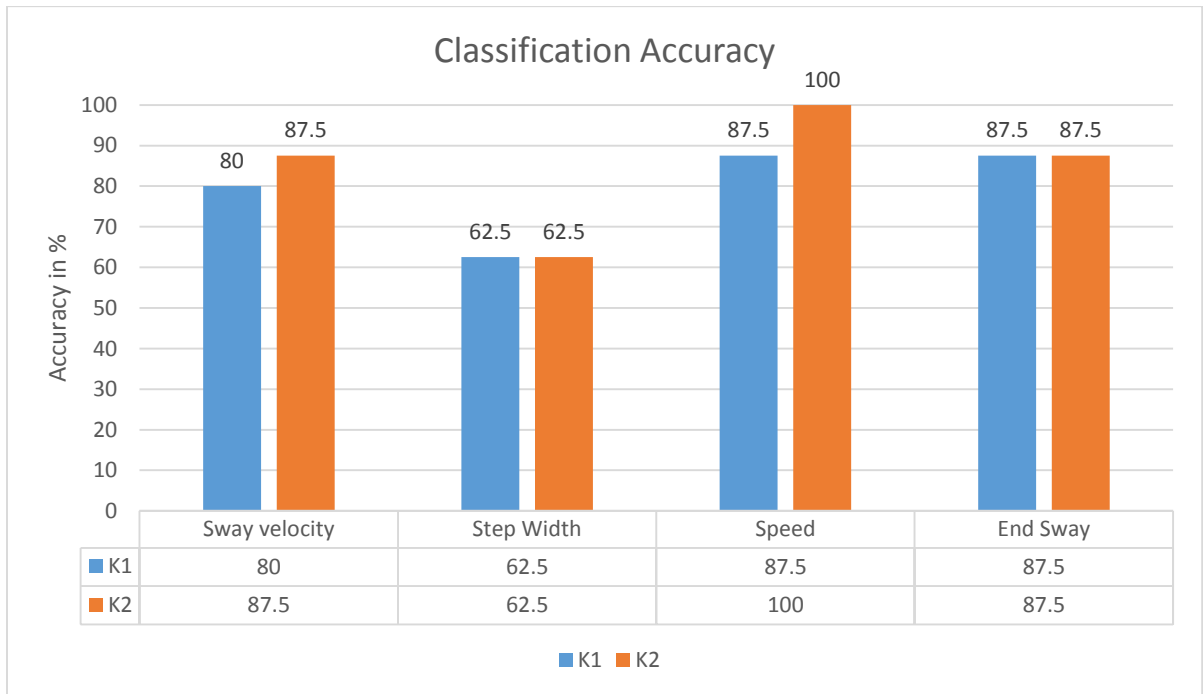


Figure 22 Classification accuracy for K1 and K2 sensors in measuring Sway Velocity, Step Width, Speed, and End Sway.

In most cases, K2 sensor performed better than K1 in measuring the biomechanical measures explained in Chapter 4 and had a larger range for activity tracking as compared to K1.

### Therapist's Ratings Compilation

In order to evaluate the IPTS, 5 older adults from Kansas City were recruited to take part in an IRB approved human subjects study. Four tests were performed using the IPTS, with a physical therapist in Columbia, MO and each subject in the home in Kansas City, MO. A survey form was used to obtain feedback about the interface and the overall system after each test, which helped to improve the system further. At the final test after development was complete, the therapist rated the technical quality of audio and video and the user satisfaction and PT interaction as high as 4.7 and 4.8 out of 5 respectively, based on 17 individual ratings in different categories. Fig. 23 and 24 show the ratings in form of bar graphs.

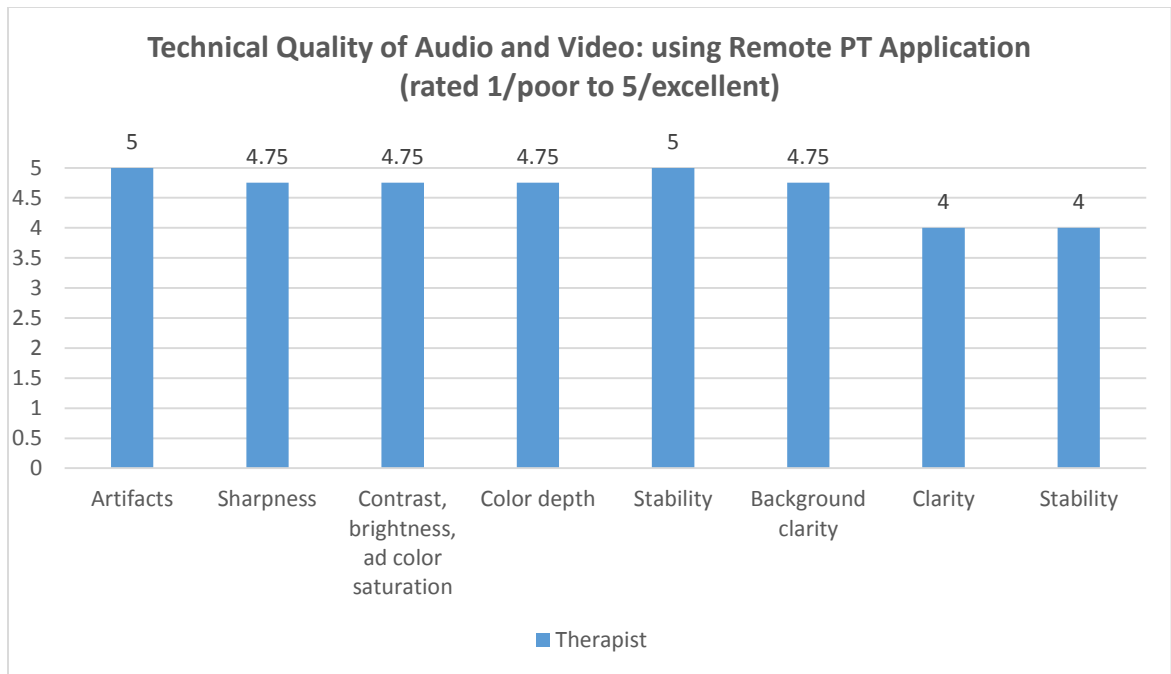


Figure 23 Technical Quality of Audio and Video: using Remote PT Application (rated 1/poor to 5/excellent).

The therapist ratings in Fig. 23 provide valuable information, stating the effectiveness of the application and its quality. The last two measures: audio clarity and stability had a lower rating because of feedback issues during the video conferencing. The feedback issues were greatly reduced using the Microsoft acoustic echo cancellation APIs. Still, because of the high sensitivity of Kinect microphone array, we heard some noise due to audio feedback.

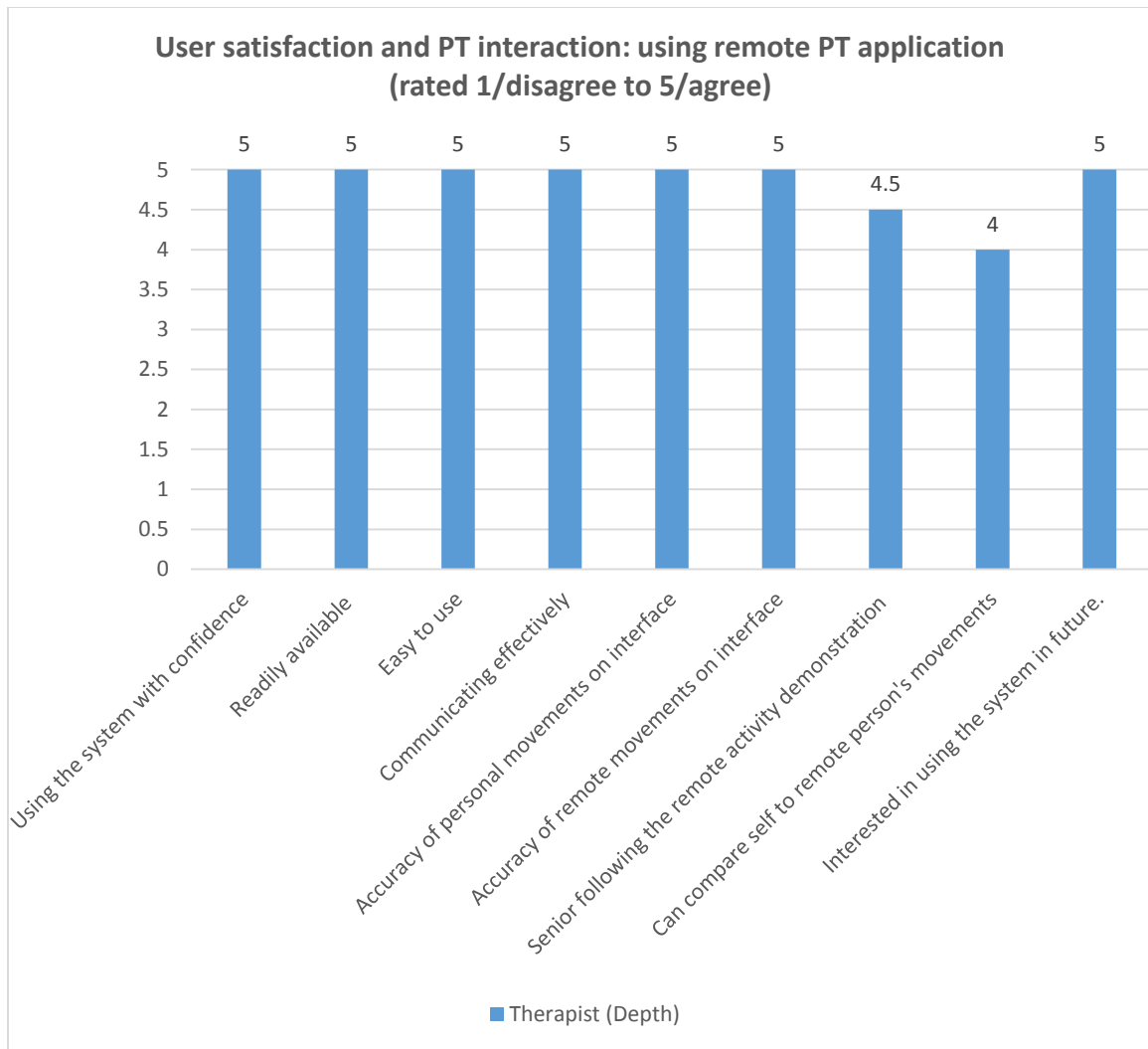


Figure 24 User satisfaction and PT interaction: using remote PT application (rated 1/disagree to 5/agree).

The application interfaces were developed with iterative feedback provided by a therapist with an active clinical practice. The ratings from Fig. 24 show a high degree of user satisfaction in almost all individual rankings.

## Chapter 6

### Conclusion

#### Contribution

We have developed a novel Kinect-based interactive PT system for remote assessment of PT clients, especially targeting older adult users. We address the problems related to conventional in-clinic PT, by providing a next generation interactive remote PT system that has potential capabilities to provide remote physical therapy to clients, especially older adults, who may find it difficult to visit the clinic. We provide two interactive interface windows with video conferencing capabilities using the Microsoft Kinect sensors those provide real-time and post-activity analysis of PT activity data. The application interfaces were developed with iterative feedback provided by a therapist with an active clinical practice using user-centered design methodology. A suitable network module was designed modifying [49] and upgrading it to the Kinect SDK compatibility version 1.8 from version 1.6 and adding features for audio data reception and audio feedback reduction.

Our second contribution is the study to validate the real-time biomechanical measures calculated using the skeletal data from the Microsoft Xbox 360 Kinect and Microsoft Xbox One Kinect, with ground truth data from a Vicon motion capture system. Good agreements were found in the validation tests. The results of this study indicate that

the Kinect skeletal models constructed by the K1 and K2 systems offer acceptable accuracy for use as a part of a remote PT system.

Our third contribution is the study to validate another set of biomechanical features measured using skeletal data from the two Kinect sensors, with ground truth data from the NeuroCom long force-plate system. In most cases, comparable agreements were found in the validation tests too. The results show potential capabilities of the inexpensive and highly portable alternative that can evaluate a PT client through capturing these biomechanical features has a great potential to augment the conventional systems. However K2 performs better in almost all cases with higher accuracy and range of human tracking. Also, the high user satisfaction ratings provided by the therapist demonstrate the potential of the system for a broader impact in future tele-health care. We also validated the full-body CoM measurements from the Kinect with the CoM and CoP measurements generated from the Vicon and the Forceplate system using the biomechanical dataset of Mizzou Motion Analysis Center, University of Missouri, Columbia, MO.

Our fourth contribution in this study is the evaluation of the usability of IPTS in real-world scenarios. Experiments were conducted 130 miles away with five independent living older adults in Kansas City, MO. At the final test after development was complete, the therapist rated the technical quality of audio and video and the user satisfaction and PT interaction as high as 4.7 and 4.8 out of 5 respectively, based on 17 individual ratings in different categories.

#### Limitation of the Study

The biggest limitation of this study is the sample size considered for different validations. It's hard to obtain a good standard deviation measurement from a small sample

size. The other limitation is the synchronization issues in the NeuroCom validation tests. The synchronization of NeuroCom and Kinect systems would have been better if we could get the raw CoP data out of the NeuroCom system to compute the results. The synchronization involved some subjective inputs and that might have enhanced the deviation of results.

Also, the GEBOD III regression equations are based on the anthropometric data of US citizens and the subjects considered for the NeuroCom validation tests were not from US. Therefore, we assume that the full-body CoM estimation may not have worked very well because the subjects were not basically from the same origin.

We could not get the foot falls accurately of any subject performing TW tests, using the Kinect's skeletal model. This issue led to higher step width errors. Whereas NeuroCom was definitely able to get the foot falls, as the subject had to walk on a force plate.

Another limitation of the Kinect system is its lower frame rate or data capturing speed. Kinect captures data at a frequency of 30 Hz whereas NeuroCom does that at 100 Hz. As we did not have the raw NeuroCom data we could never resample it to 30 Hz.

Moreover, Kinect provides a very noisy skeletal data when any of the joints are occluded. In TW tests, the foot behind the front foot is always occluded and the foot joint at the back always had a very high noise associated with it.

The high average percentage deviation in the validation test results in NeuroCom validation shows possible synchronization issues. The NeuroCom estimates CoG from CoP measurements so we assume that the comparison between the two different estimations

(CoM estimation from the Kinects and CoG estimations from the NeuroCom) might have caused the high deviations measures.

### Future Work

Our future work will consider feedback from a larger group of PT clients and therapists to make the user experience better. A larger sample size will be considered for the future validations. More validation tests will be conducted including other functional limitations tests provided by the NeuroCom system.

The algorithm for step width calculation can be improved for better accuracy.

The PT application currently uses just K1 and can be upgraded to support K2 sensor, which can provide a stable and wider range for activity detection using Kinect skeletal models.

The application currently used TCP sockets for data communication. The network part can be implemented with UDP sockets for a better network performance. The Kinect data can also be encrypted for secure data transfer.

Currently the system requires the two end computers to have public IPs to communicate with each other. In those cases where we can not avail a public network domain, VPN network connections can be used. Methods such as STUN and NAT traversal can be implemented for better data communication channel systems.

Currently the application is only compatible with Microsoft Windows and resolutions: 1080p and 720p. The interfaces can be improved providing compatibility with different screen resolutions and operating systems.

We provided a quick solution to the audio feedback issue using Microsoft libraries that works well in specific conditions, which may not be sufficient for some scenarios, such as, auditoriums. Advanced hardware or software audio feedback solutions can be used to fix this issue.

We are currently developing a stand-alone version of the application for the PT clinic, at the request of our PT collaborator.

## Bibliography

- [1] M. D. Landry, Thomas C Ricketts, E. Fraher, and M. C. Verrier, "Physical Therapy Health Human Resource Ratios: A Comparative Analysis of the United States and Canada," *Physical Therapy*, pp. 149-161, 2009.
- [2] A. Seppälä, P. Nykänen, and P. Ruotsalainen, "Development of Personal Wellness Information Model for Pervasive Healthcare," *Journal of Computer Networks and Communications*, vol. 2012, p. 10, 2012.
- [3] S. McMahon and J. Fleury, "Wellness in Older Adults: A Concept Analysis," *Nurs Forum*, vol. 47, 2012.
- [4] M. Skubic, "Assessing Mobility and Cognitive Problems in Elders," in *AAAI Fall 2005 Symposium Workshop on Caring Machines: AI in Eldercare*, Arlington, Virginia, 2005, pp. 4-6.
- [5] G. Demiris, M. Skubic, M. Rantz, K. Courtney, M. Aud, H. Tyrer, *et al.*, "Facilitating Interdisciplinary Design Specification of "Smart Homes" for Aging in Place," in *International Congress of the European Federation of Medical Informatics*, Maastricht, Netherlands, 2006, pp. 44-50.
- [6] P. Takahashi, G. Hanson, J. Pecina, R. Stroebel, R. Chaudhry, N. Shah, *et al.*, "A randomized controlled trial of telemonitoring in older adults with multiple chronic conditions: the Tele-ERA study," *BMC Health Services Research*, 2010.
- [7] J. Pecina, G. Hanson, H. H. Van, and P. Takahashi, "Impact of telemonitoring on older adults health-related quality of life: the Tele-ERA study," *Quality of Life Research*, vol. 22, 2013.
- [8] D. Tacconi, R. Tomasi, C. Costa, and O. Mayora, "A system for remote orthopedics rehabilitation," in *Pervasive Computing Technologies for Healthcare (PervasiveHealth), 2013 7th International Conference on*, 2013, pp. 313-314.
- [9] M. Pickerill and R. Harter, "Validity and reliability of limits-of-stability testing: a comparison of 2 postural stability evaluation devices," *J Athl Train*, vol. 46, pp. 600-606, 2011
- [10] T. Chien Ming, L. Chung Liang, D. Erdenetsogt, and C. Yung-Fu, "A Microsoft Kinect Based Virtual Rehabilitation System," in *Computer, Consumer and Control (IS3C), 2014 International Symposium on*, 2014, pp. 934-937.
- [11] C. Camporesi, M. Kallmann, and J. J. Han, "VR solutions for improving physical therapy," in *Virtual Reality (VR), 2013 IEEE*, 2013, pp. 77-78.
- [12] M. Patanapanich, V. Vanijja, and P. Dajpratham, "Self-physical rehabilitation system using the microsoft kinect," in *Information Technology Systems and Innovation (ICITSI), 2014 International Conference on*, 2014, pp. 241-247.
- [13] R. N. Madeira, L. Costa, and O. Postolache, "PhysioMate - Pervasive physical rehabilitation based on NUI and gamification," in *Electrical and Power Engineering (EPE), 2014 International Conference and Exposition on*, 2014, pp. 612-616.
- [14] M. H. Abd Latif, H. M. Yusof, S. N. Sidek, M. S. Shikhrabi, and M. H. Safie, "A gaming-based system for stroke patients physical rehabilitation," in *Biomedical*

- Engineering and Sciences (IECBES), 2014 IEEE Conference on*, 2014, pp. 690-695.
- [15] D. Sadihov, B. Migge, R. Gassert, and K. Yeongmi, "Prototype of a VR upper-limb rehabilitation system enhanced with motion-based tactile feedback," in *World Haptics Conference (WHC), 2013*, 2013, pp. 449-454.
  - [16] C. Schonauer, T. Pintaric, H. Kaufmann, S. Jansen - Kosterink, and M. Vollenbroek-Hutten, "Chronic pain rehabilitation with a serious game using multimodal input," in *Virtual Rehabilitation (ICVR), 2011 International Conference on*, 2011, pp. 1-8.
  - [17] J. Nielsen, "Iterative user-interface design," *Computer*, vol. 26, pp. 32-41, 1993.
  - [18] W. Buxton and R. Sniderman, "Iteration in the Design of the Human-Computer Interface," in *Proceedings of the 13th Annual Meeting, Human Factors Association of Canada*, 1980, pp. 72-81.
  - [19] D. Travis, *The Fable of the User-Centred Designer: Userfocus*, 2009
  - [20] J. M. Carroll, "Five reasons for scenario-based design," *Interacting with Computers*, vol. 13, 2000.
  - [21] MA Livingston, J Sebastian, Z Ai, and J. Decker, "Performance Measurements of the Microsoft Kinect Skeleton," in *Virtual Reality Short Papers and Posters (VRW)*, 2012.
  - [22] K. LaBelle, "Evaluation of Kinect Joint Tracking for Clinical and InHome Stroke Rehabiliatoin Tools," Undergraduate Thesis, University of Notre Dame, 2011.
  - [23] T. Dutta, "Evaluation of the Kinect sensor for 3-D kinematic measurement in the workplace," *Applied Ergonomics*, vol. 43, pp. 645-649, 2012.
  - [24] R. A. Clark, Y.-H. Pua, K. Fortin, C. Ritchie, Kate E. Webster, L. Denehy, *et al.*, "Validity of the Microsoft Kinect for assessment of postural control," *Gait & Posture*, vol. 36, pp. 372-377, 2012.
  - [25] B. B. re, B. Jansen, P. Salvia, H. Bouzahouene, L. Omelina, F. Moiseev , *et al.*, "Validity and reliability of the Kinect within functional assessment activities: Comparison with standard stereophotogrammetry," *Gait & Posture*, vol. 39, pp. 593-598, 2014.
  - [26] J. Fasola and M. Mataric, "A Socially Assistive Robot Exercise Coach for the Elderly," *Journal of Human-Robot Interaction*, vol. 2, pp. 3-32, 2013.
  - [27] S. Obdr?lek, G. Kurillo, E. Seto, and R. Bajcsy, "Architecture of an Automated Coaching System for Elderly Population," in *Proc. of MMVR, 2013*, 2013.
  - [28] Y. Chen and Y. Hung, "Using Real-time Acceleration Data for Exercise Movement Training with a Decision Tree Approach," in *IEEE Conference on Machine Learning and Cybernetics, 2009*, 2009.
  - [29] K. Huang, P. Sparto, S. Kiesler, and D. Siewiorek, "iPod for Home Balance Rehabilitation Exercise Monitoring," in *IEEE Symposium on Wearable Computers, 2012*.
  - [30] P. A. Hageman, J. M. Leibowitz, and D. Blanke, "Age and gender effects on postural control measures," *Archives of Physical Medicine and Rehabilitation*, vol. 76, pp. 961-965, 1995.
  - [31] S. Niam, W. Cheung, P. E. Sullivan, S. Kent, and X. Gu, "Balance and physical impairments after stroke," *Archives of Physical Medicine and Rehabilitation*, vol. 80, pp. 1227-1233, 1999.

- [32] K. M. Guskiewicz and D. H. Perrin, "Research and Clinical Applications of Assessing Balance " *Journal of Sport Rehabilitation*, pp. 45-63, 1996.
- [33] P. Goldie , T. Bach, and Evans, "Force platform measures for evaluating postural control: Reliability and validit," *Arch. Phys. Med. Rehabil.* , vol. 70, pp. 510-517, 1989.
- [34] NeuroCom. (2012). *ABOUT NEUROCOM, A DIVISION OF NATUS*. Available: <http://resourcesonbalance.com/neurocom/about/index.aspx>
- [35] Goldie PA, Evans OM, and B. TM, " Steadiness in One-Legged Stance: Development of Reliable Force- Platform Testing Procedure," *Arch Phys Med Rehabil*, vol. 73, 1992.
- [36] Goldie PA, Evans OM, and B. TM, "Postural control following inversion injuries of the ankle.," *Arch Phys Med Rehabil*, vol. 75, pp. 969-975, 1994.
- [37] Hu MH, Ho HC, and W. JS, "Comparisons of Dynamic CDP/Computerized Dynamic Posturography and One-Leg Stance in elite college athletes," *FJPT*, vol. 30, pp. 33-40, 2005.
- [38] Taylor EL, Williams MD, Bemben MG, and S. RL, " Association between field and laboratory tests of postural balance and sway in older adults," *Medicine & Science in Sports & Exercise*, vol. 34, 2002.
- [39] Vaara M and K. SL, "Reliability of functional balance tests measured with posturography in healthy adults," *World Congress of Physical Therapy*, 2007.
- [40] Cambier D, Cools A, Danneels L, and W. W, "Reference Data for 4-and 5-year-old-Children on the Balance Master: Values and Clinical Feasibility," *Eur J Pediatr*, vol. 160, pp. 317-322, 2001.
- [41] Wikipedia. (2015). *Balance (ability)*. Available: [http://en.wikipedia.org/wiki/Balance\\_\(ability\)](http://en.wikipedia.org/wiki/Balance_(ability))
- [42] J. Sell and P. O'Connor, "The Xbox One System on a Chip and Kinect Sensor," *Micro, IEEE*, vol. 32, pp. 44-53, 2014.
- [43] M. Corporation, "Kinect for Windows SDK 2.0 Documentation," 2014.
- [44] M. Corporation, "Kinect for Windows SDK 1.8 Documentation," 2012.
- [45] S. Bhimji, "Static and Dynamic Accuracy of the VICON 370 3-D Kinematic System," *Gait Posture*, vol. 11, p. 130, 2000.
- [46] K. E. Webster, J. E. Wittwer, and J. A. Feller, "Validity of the GAITRite® Walkway System for the Measurement of Averaged and Individual Step Parameters of Gait," *Gait & Posture*, vol. 22, pp. 317-321, 2005.
- [47] W. H. Organization, "International Classification of Disease, 9th rev. Clinical Modification," 1997.
- [48] W. H. Organization, "ICDIIH-2 International Classification of Function and Disability. Beta-2 draft. Short Version.," 19999.
- [49] Crutkas, Danielfe, and Peekb, "Coding4Fun Kinect Service v1.6 Documentation," 2012.
- [50] M. Corp. *System.Speech Namespaces documentation for .NET Framework 4.5*
- [51] M. E. Gross, "The GEBOD III Program User's Guide and Description," Air Force Systems Command Wright-Patterson Air Force Base, Ohio 45433-65731991.

- [52] L. F. Yeung, K. C. Cheng, C. H. Fong, W. C. C. Lee, and K.-Y. Tong, "Evaluation of the Microsoft Kinect as a clinical assessment tool of body sway," *Gait & Posture*, vol. 40, pp. 532-638, 2014.
- [53] Prasad Calyam, Anup Mishra, Ronny Bazan, Dmitrii Chemodanov, Alex Berryman, Kunpeng Zhu, *et al.*, "Synchronous Big Data Analytics for Personalized and Remote Physical Therapy," *Elsevier Journal of Pervasive and Mobile Computing*, 2014.
- [54] J. T. McConville, I. Churchill, I. K, C. E. Clauser, and J. Cuzzi, "Anthropometric Relationships of Body and Body Segment Moment of Inertia," Aerospace Medical Research Laboratory, Wright-Patterson Air Force Base, Ohio 1989.
- [55] Young, J. W., R. F., C. C. Chandler, K. M. R., G. F. Z., *et al.*, "Anthropometric and Mass Distribution Characteristics of the Adult Female," Civil Aeromedical Institute, Federal Aviation Administration, Oklahoma City, Oklahoma, 1983.
- [56] (2015). *Center of mass*. Available: [http://en.wikipedia.org/wiki/Center\\_of\\_mass#Center\\_of\\_gravity](http://en.wikipedia.org/wiki/Center_of_mass#Center_of_gravity)

## Appendix A

### CoG and CoM traces for NeuroCom validation test

The NeuroCom validation section comprises samples of CoM and CoG traces from the Kinects and NeuroCom system, respectively. In this section, all the CoM plots measured from the Kinect sensors are compared with the NeuroCom CoG plots, for the four subjects including three trials for each of the tests: single leg stance with eyes open (SLS EO), single leg stance with eyes closed (SLS EC), tandem walk with eyes open (TW EO), and tandem walk with eyes closed (TW EC). Size of each horizontal trace for TW is 1.2 m X .05 m whereas it is 0.5 m X 0.5 m for SLS traces.

In some cases the NeuroCom plots are more detailed because of the higher sampling frequency (100 Hz) of NeuroCom forceplate system as compared to K1 and K2 (30 Hz).

Test results for Subject 1

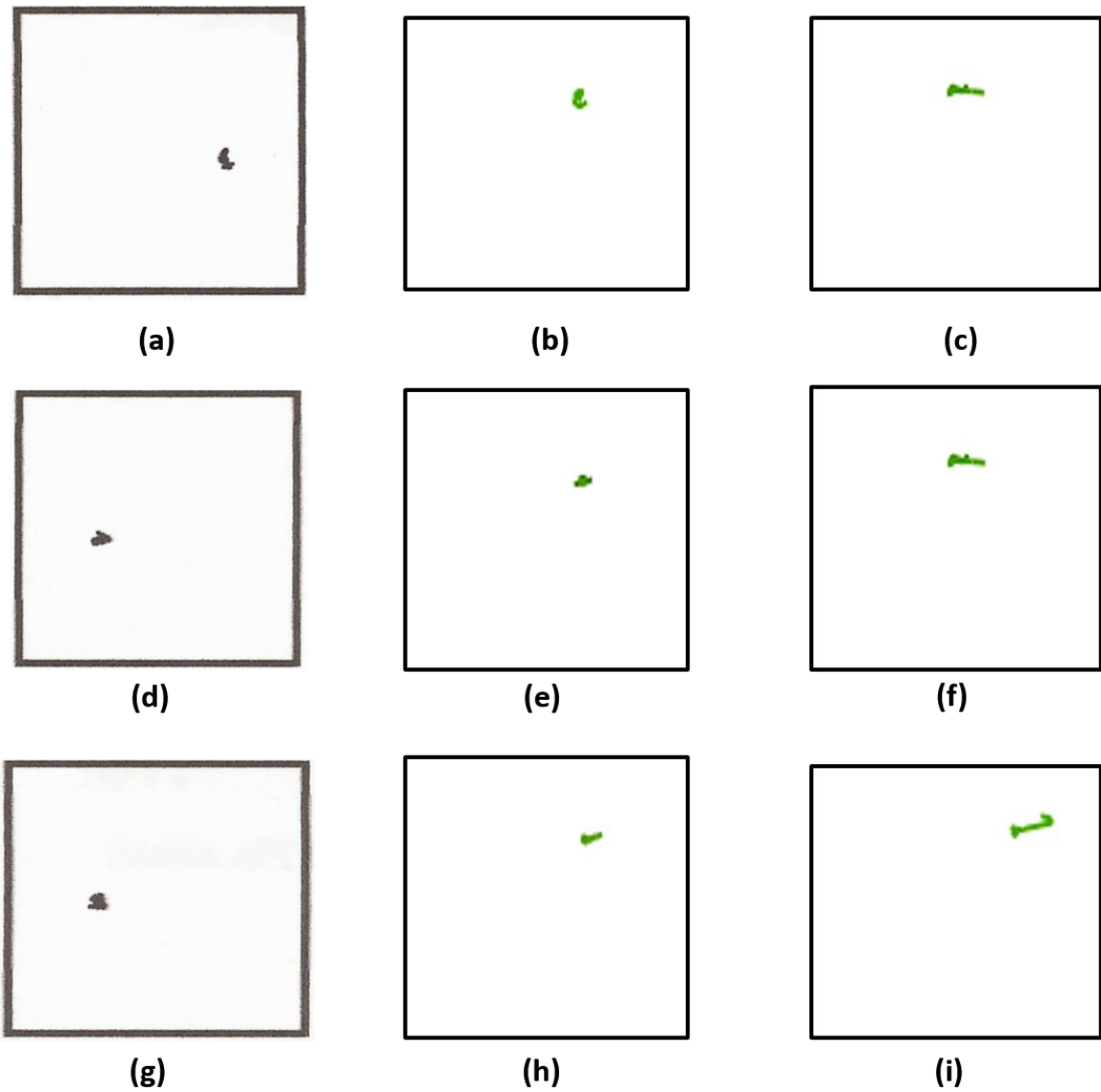


Figure 25 Subject 1- SLS eyes open test results. Trial 1: (a) NeuroCom CoG plot; (b) K1 CoM plot; (c) K2 CoM plot; Trial 2: (d) NeuroCom CoG plot; (e) K1 CoM plot; (f) K2 CoM plot; Trial 3: (g) NeuroCom CoG plot; (h) K1 CoM plot; (i) K2 CoM plot.

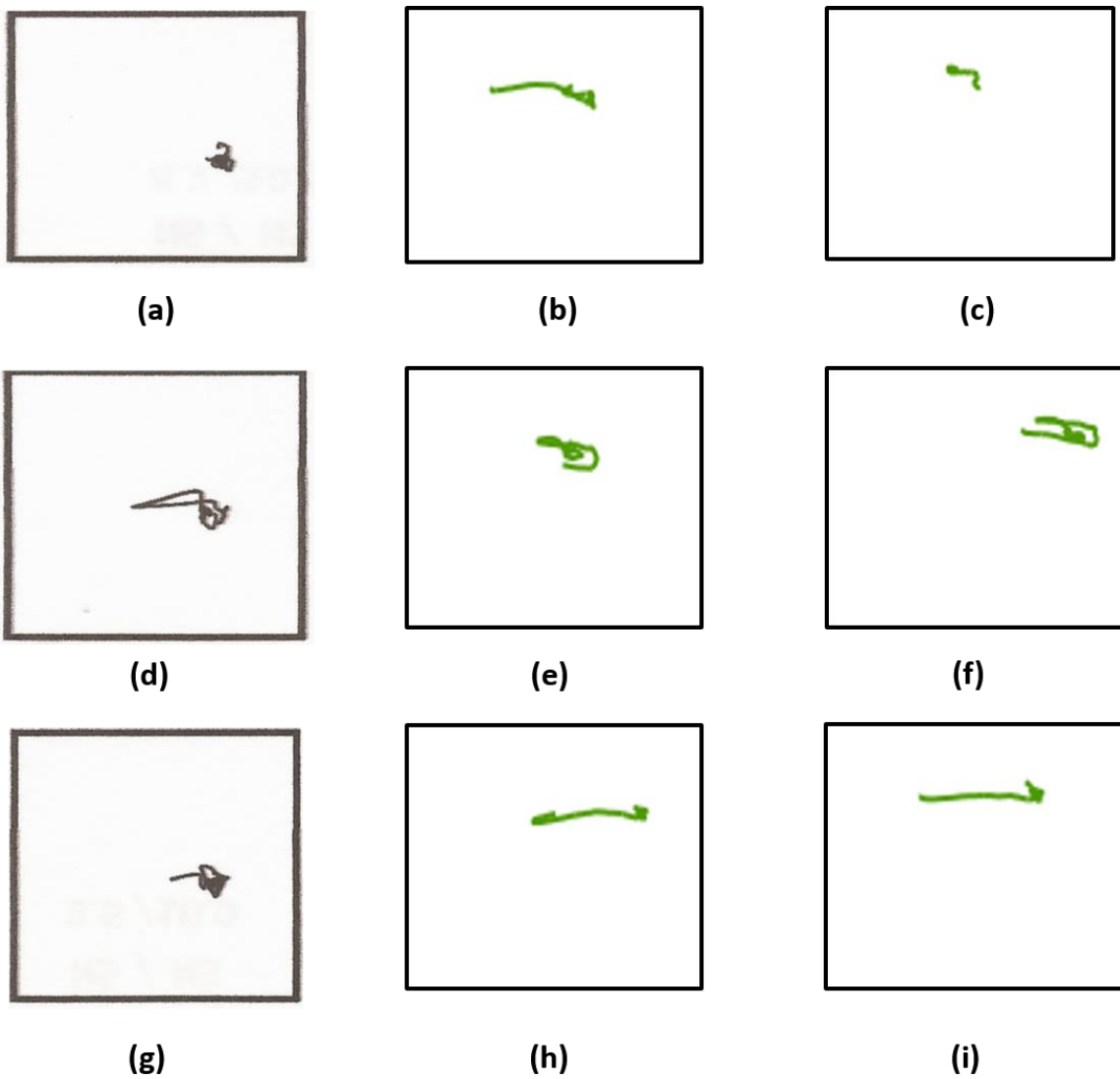
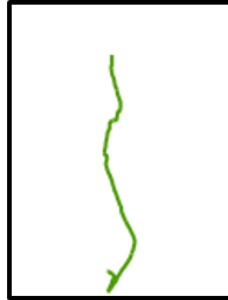


Figure 26 Subject 1- SLS eyes closed test results. Trial 1: (a) NeuroCom CoG plot; (b) K1 CoM plot; (c) K2 CoM plot; Trial 2: (d) NeuroCom CoG plot; (e) K1 CoM plot; (f) K2 CoM plot; Trial 3: (g) NeuroCom CoG plot; (h) K1 CoM plot; (i) K2 CoM plot.



**(a)**



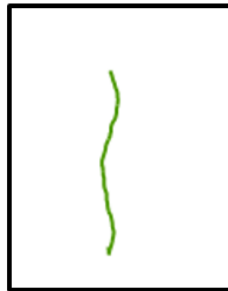
**(b)**

Data Missing

**(c)**



**(d)**



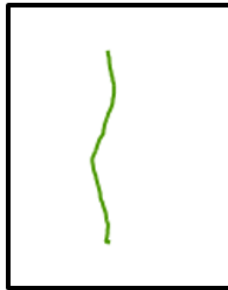
**(e)**

Data Missing

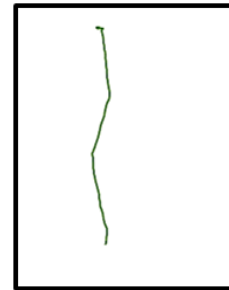
**(f)**



**(g)**



**(h)**



**(i)**

Figure 27 Subject 1- TW eyes open test results. Trial 1: (a) NeuroCom CoG plot; (b) K1 CoM plot; (c) K2 CoM plot; Trial 2: (d) NeuroCom CoG plot; (e) K1 CoM plot; (f) K2 CoM plot; Trial 3: (g) NeuroCom CoG plot; (h) K1 CoM plot; (i) K2 CoM plot.

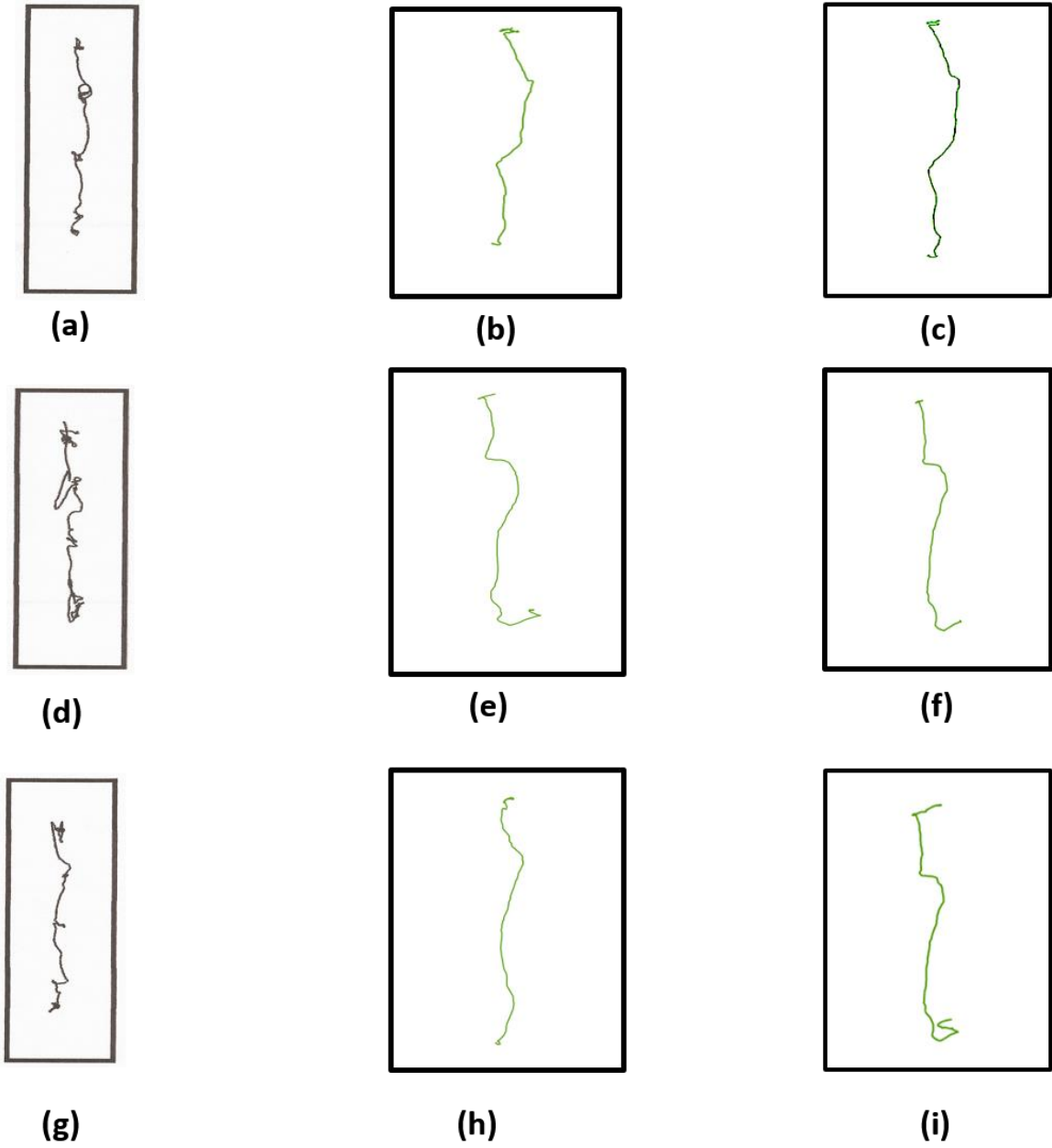


Figure 28 Subject 1- TW eyes closed test results. Trial 1: (a) NeuroCom CoG plot; (b) K1 CoM plot; (c) K2 CoM plot; Trial 2: (d) NeuroCom CoG plot; (e) K1 CoM plot; (f) K2 CoM plot; Trial 3: (g) NeuroCom CoG plot; (h) K1 CoM plot; (i) K2 CoM plot.

Test results for Subject 2

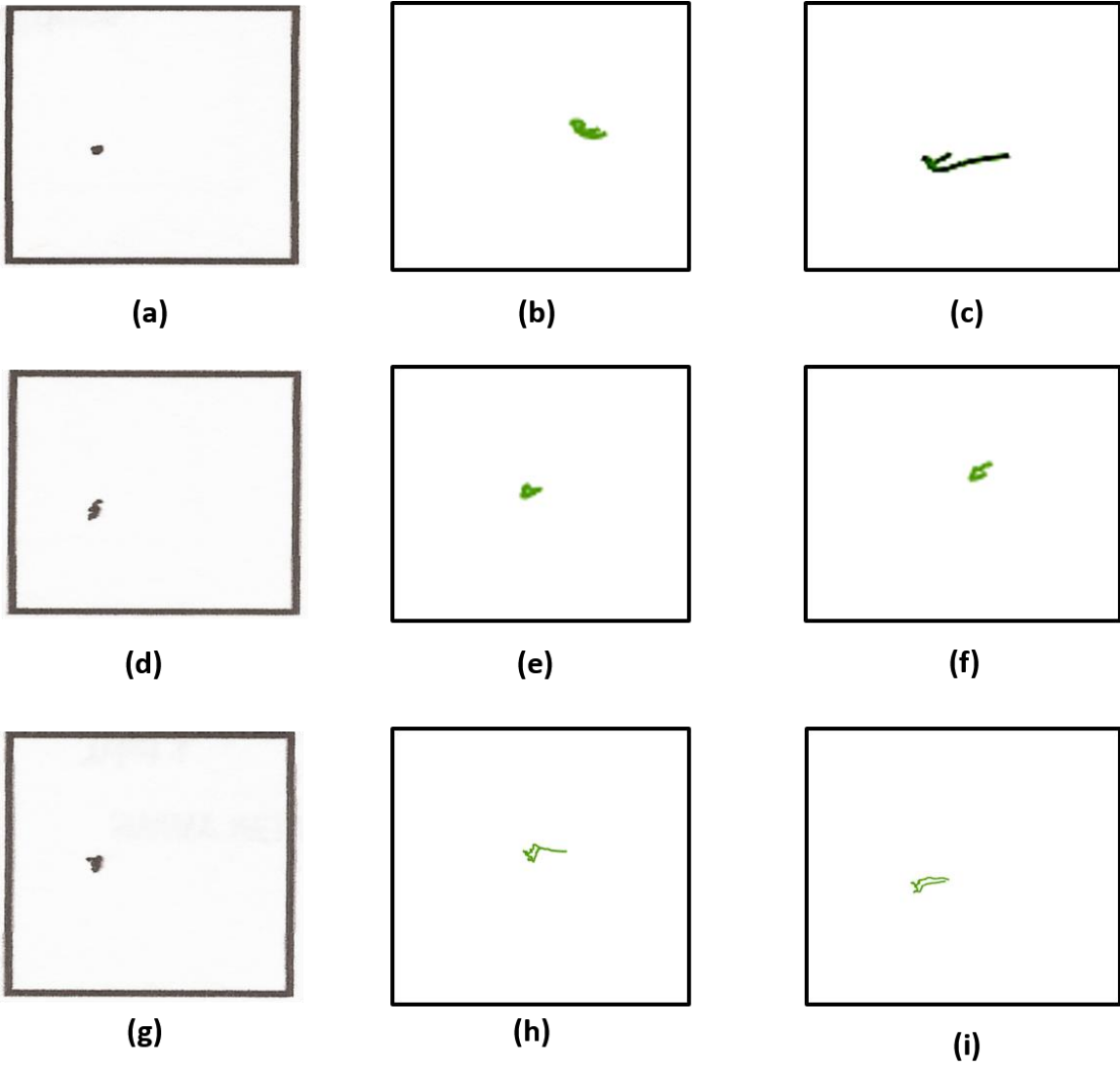


Figure 29 Subject 2- SLS eyes open test results. Trial 1: (a) NeuroCom CoG plot; (b) K1 CoM plot; (c) K2 CoM plot; Trial 2: (d) NeuroCom CoG plot; (e) K1 CoM plot; (f) K2 CoM plot; Trial 3: (g) NeuroCom CoG plot; (h) K1 CoM plot; (i) K2 CoM plot.

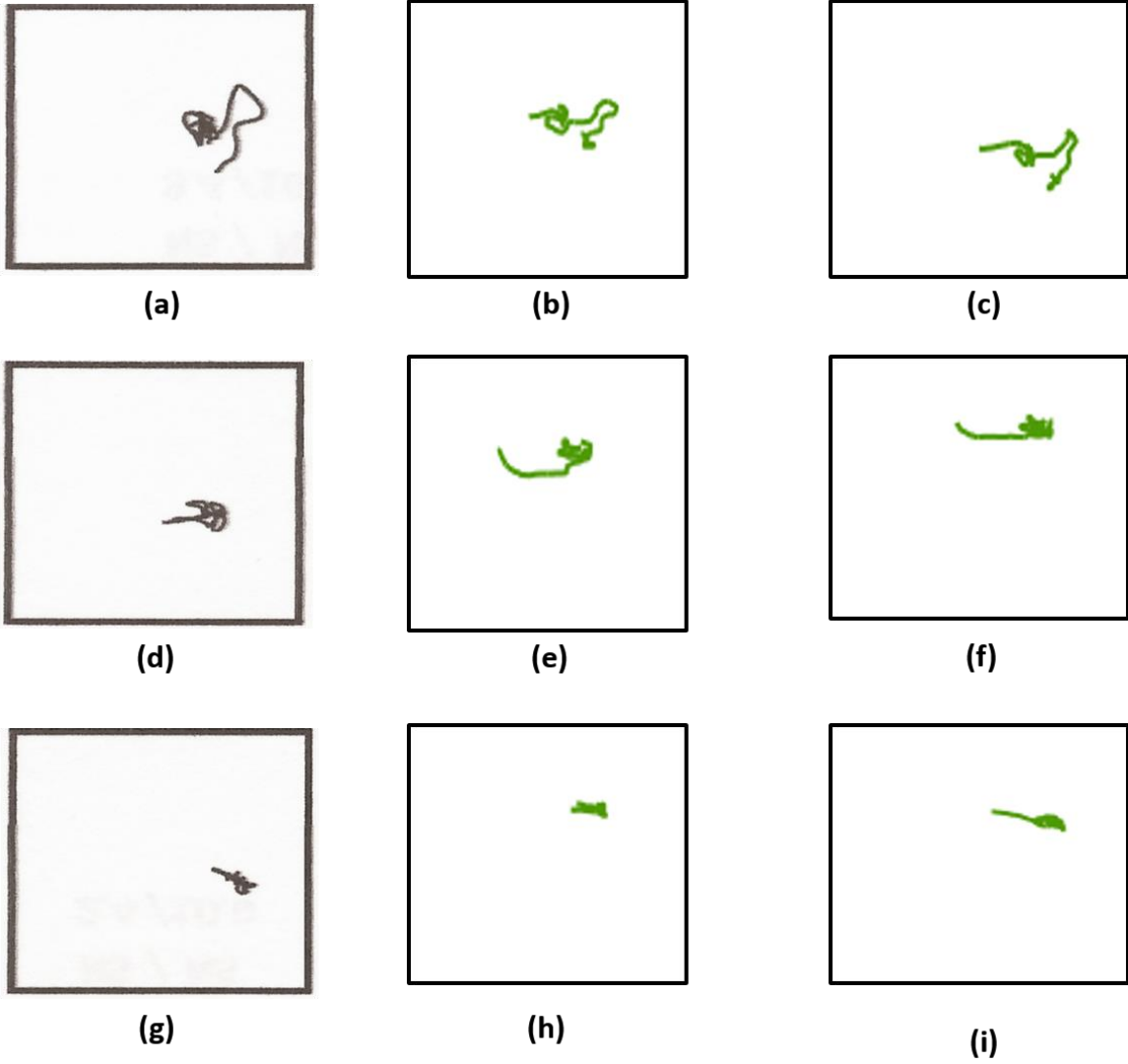


Figure 30 Subject 2- SLS eyes closed test results. Trial 1: (a) NeuroCom CoG plot; (b) K1 CoM plot; (c) K2 CoM plot; Trial 2: (d) NeuroCom CoG plot; (e) K1 CoM plot; (f) K2 CoM plot; Trial 3: (g) NeuroCom CoG plot; (h) K1 CoM plot; (i) K2 CoM plot.

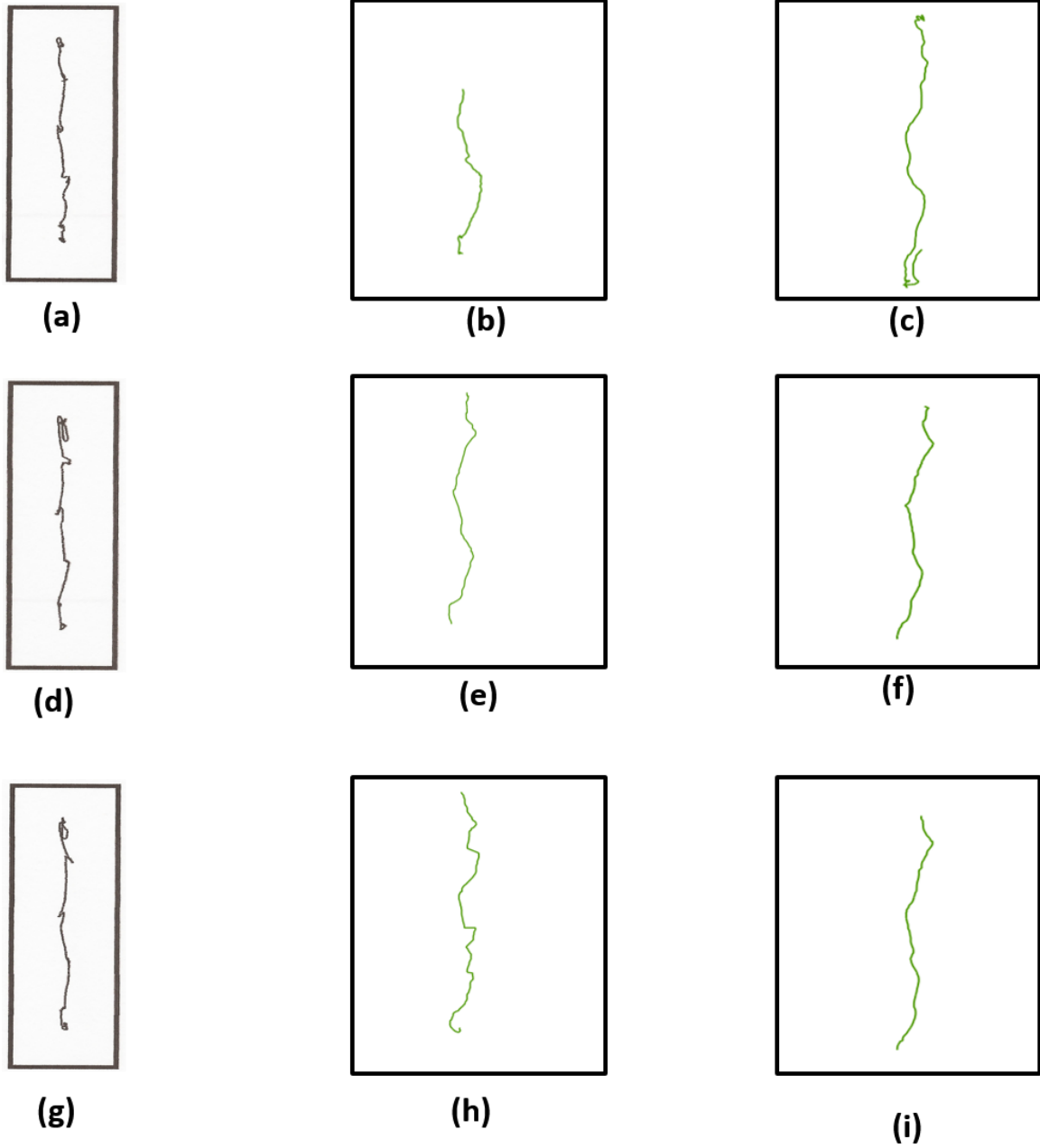


Figure 31 Subject 2- TW eyes open test results. Trial 1: (a) NeuroCom CoG plot; (b) K1 CoM plot; (c) K2 CoM plot; Trial 2: (d) NeuroCom CoG plot; (e) K1 CoM plot; (f) K2 CoM plot; Trial 3: (g) NeuroCom CoG plot; (h) K1 CoM plot; (i) K2 CoM plot.

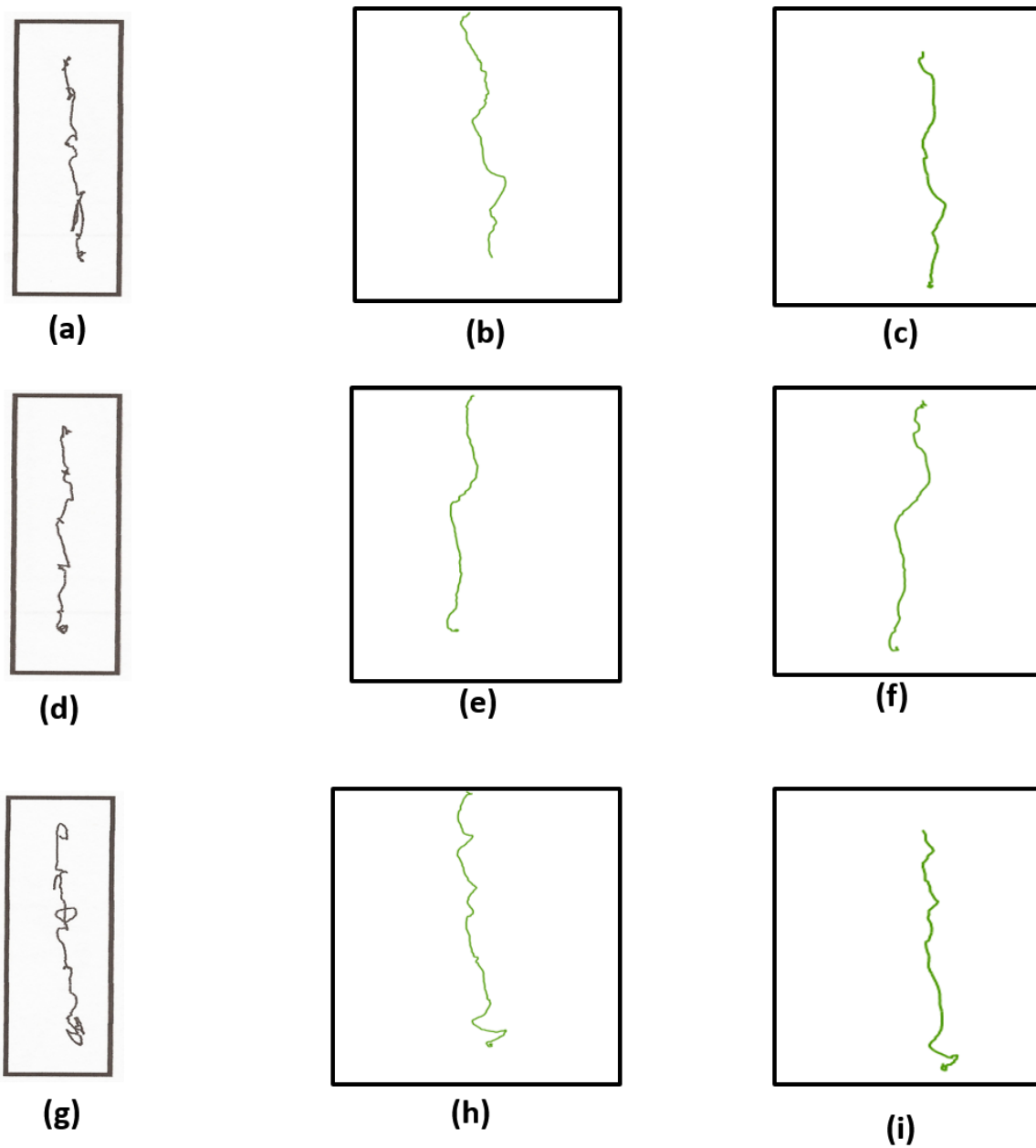


Figure 32 Subject 2- TW eyes closed test results. Trial 1: (a) NeuroCom CoG plot; (b) K1 CoM plot; (c) K2 CoM plot; Trial 2: (d) NeuroCom CoG plot; (e) K1 CoM plot; (f) K2 CoM plot; Trial 3: (g) NeuroCom CoG plot; (h) K1 CoM plot; (i) K2 CoM plot.

Test results for Subject 3

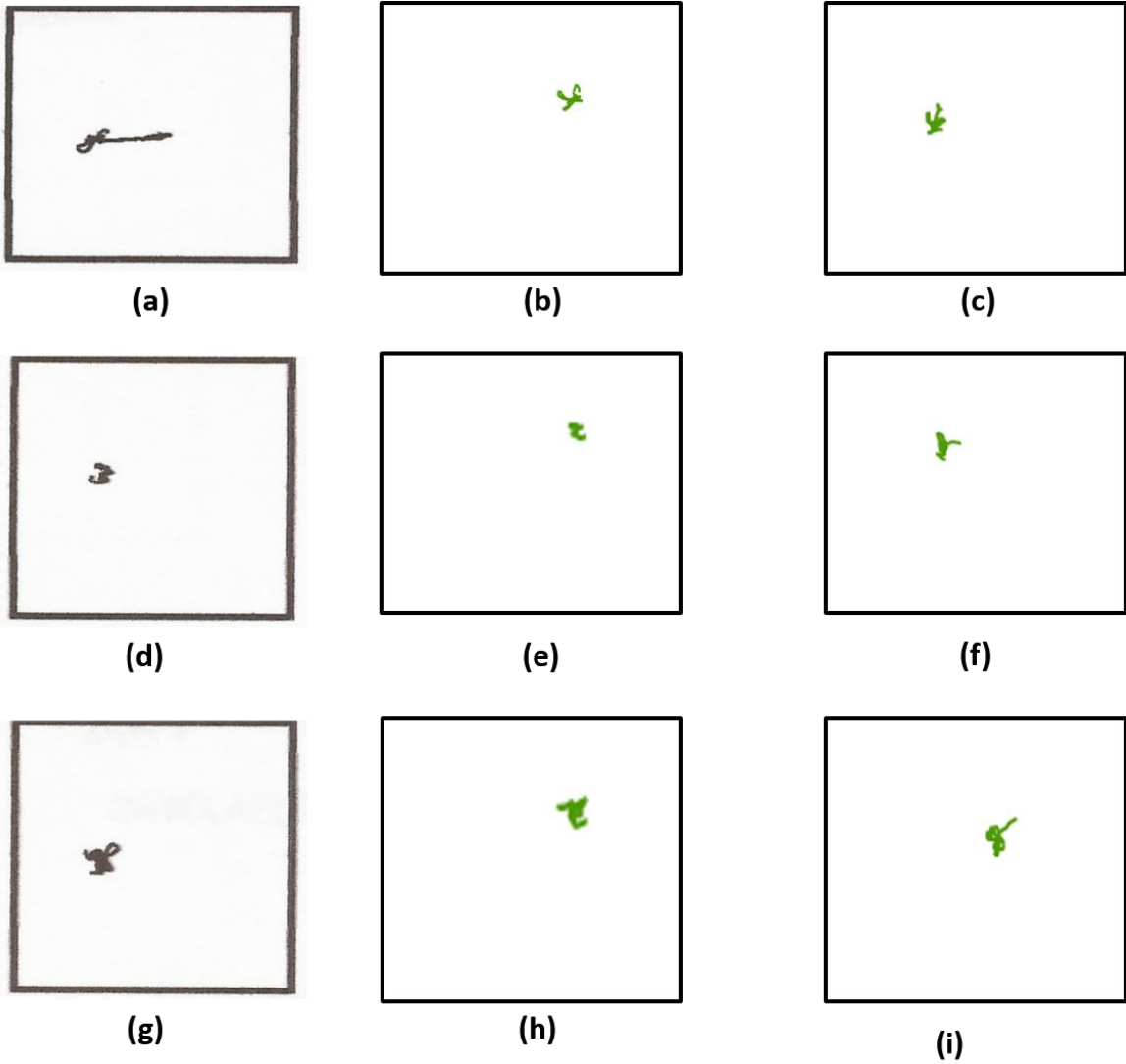


Figure 33 Subject 3- SLS eyes open test results. Trial 1: (a) NeuroCom CoG plot; (b) K1 CoM plot; (c) K2 CoM plot; Trial 2: (d) NeuroCom CoG plot; (e) K1 CoM plot; (f) K2 CoM plot; Trial 3: (g) NeuroCom CoG plot; (h) K1 CoM plot; (i) K2 CoM plot.

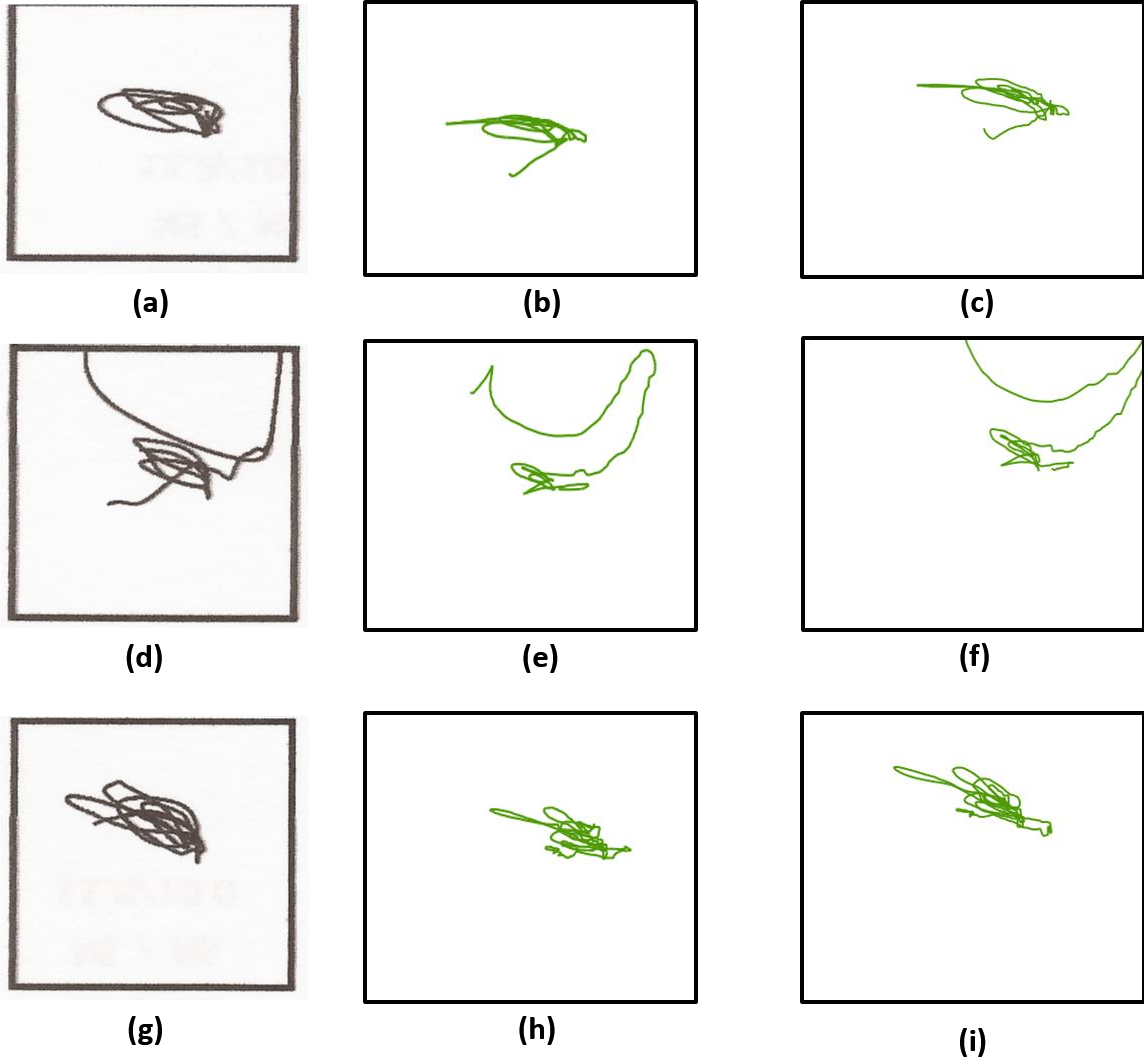


Figure 34 Subject 3- SLS eyes closed test results. Trial 1: (a) NeuroCom CoG plot; (b) K1 CoM plot; (c) K2 CoM plot; Trial 2: (d) NeuroCom CoG plot; (e) K1 CoM plot; (f) K2 CoM plot; Trial 3: (g) NeuroCom CoG plot; (h) K1 CoM plot; (i) K2 CoM plot.

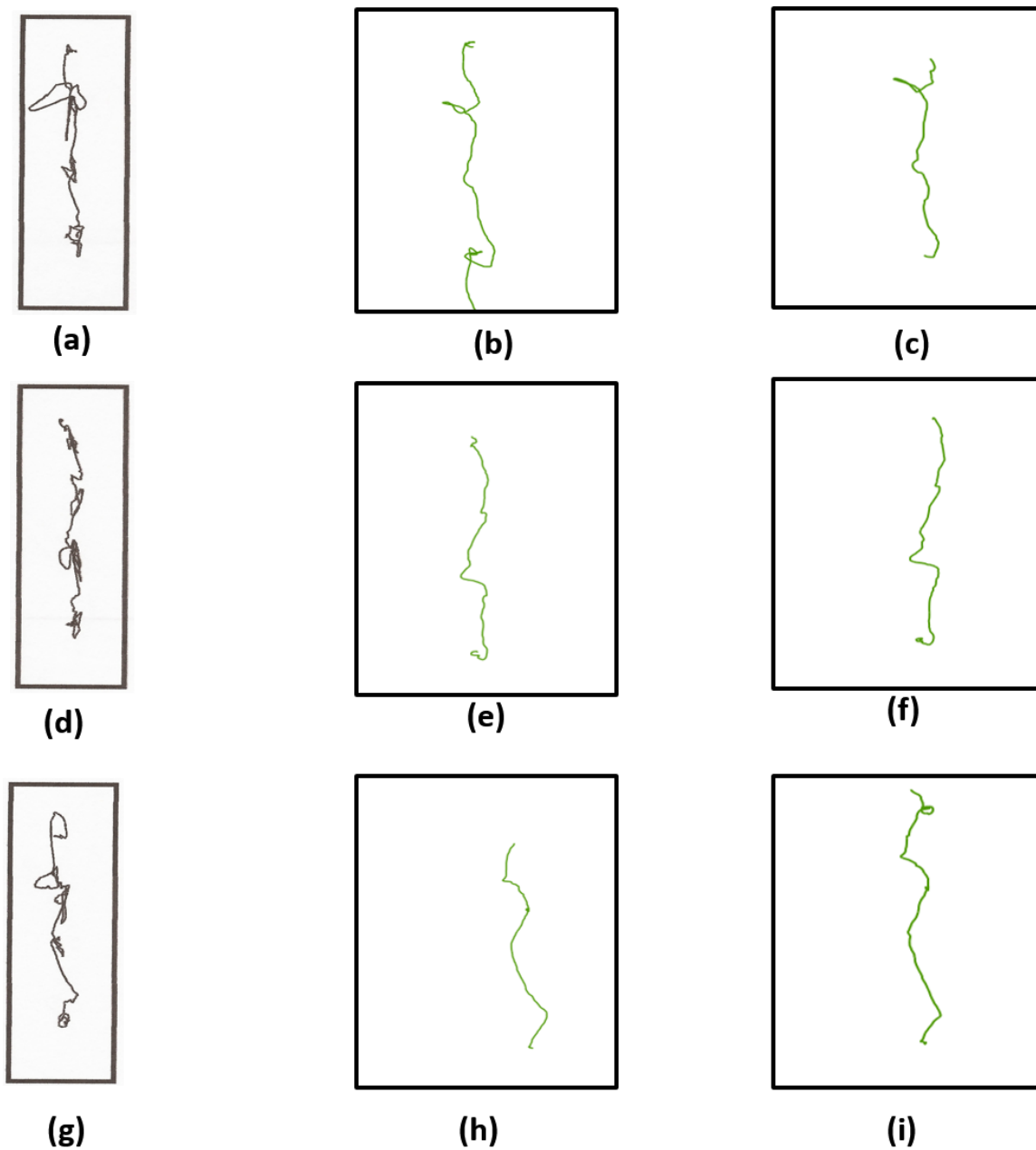
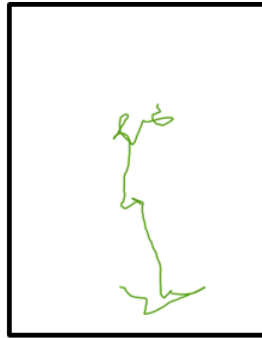


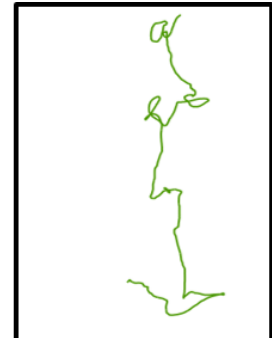
Figure 35 Subject 3- TW eyes open test results. Trial 1: (a) NeuroCom CoG plot; (b) K1 CoM plot; (c) K2 CoM plot; Trial 2: (d) NeuroCom CoG plot; (e) K1 CoM plot; (f) K2 CoM plot; Trial 3: (g) NeuroCom CoG plot; (h) K1 CoM plot; (i) K2 CoM plot.



**(a)**



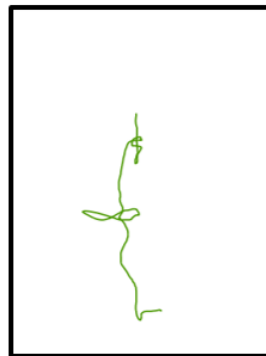
**(b)**



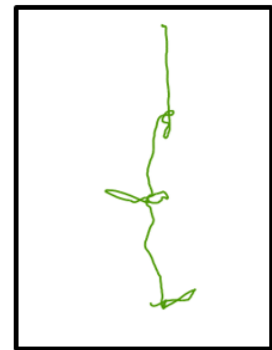
**(c)**



**(d)**



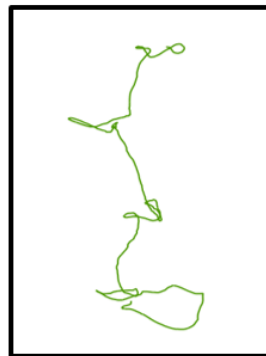
**(e)**



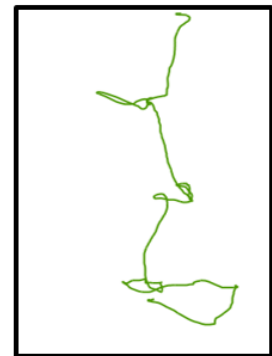
**(f)**



**(g)**



**(h)**



**(i)**

Figure 36 Subject 3- TW eyes closed test results. Trial 1: (a) NeuroCom CoG plot; (b) K1 CoM plot; (c) K2 CoM plot; Trial 2: (d) NeuroCom CoG plot; (e) K1 CoM plot; (f) K2 CoM plot; Trial 3: (g) NeuroCom CoG plot; (h) K1 CoM plot; (i) K2 CoM plot.

Test results for Subject 4

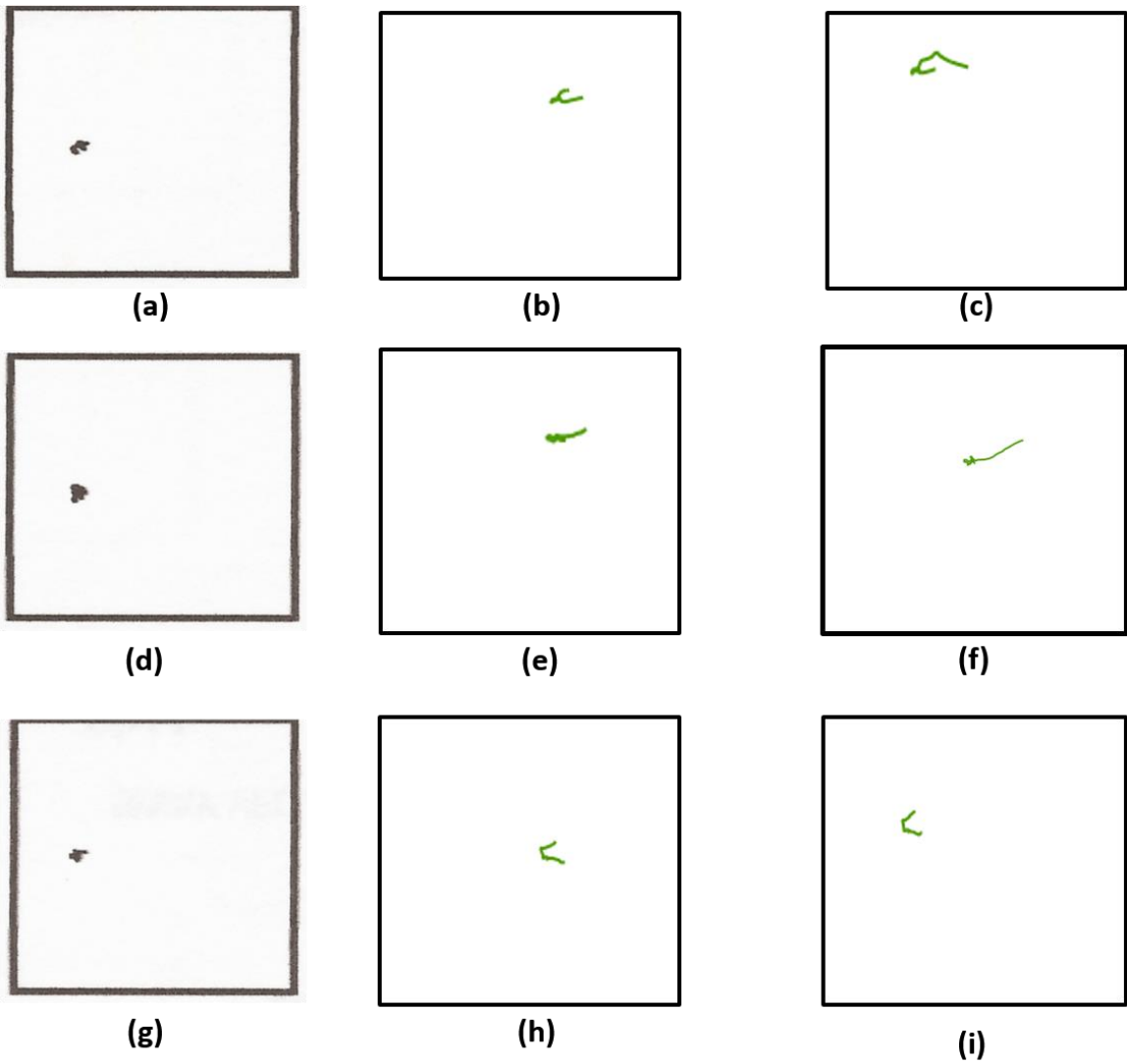


Figure 37 Subject 4- SLS eyes open test results. Trial 1: (a) NeuroCom CoG plot; (b) K1 CoM plot; (c) K2 CoM plot; Trial 2: (d) NeuroCom CoG plot; (e) K1 CoM plot; (f) K2 CoM plot; Trial 3: (g) NeuroCom CoG plot; (h) K1 CoM plot; (i) K2 CoM plot.

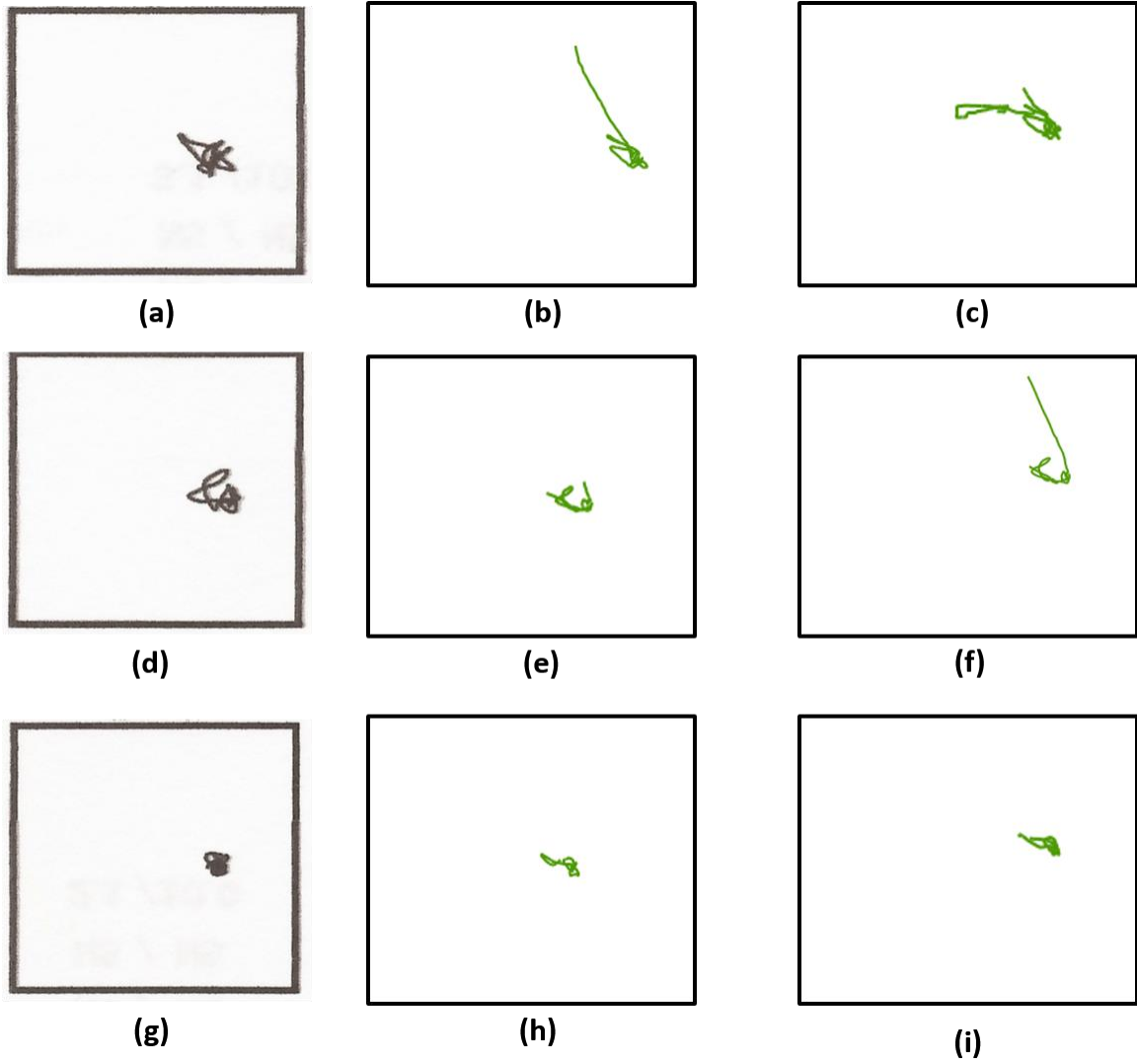


Figure 38 Subject 4- SLS eyes closed test results. Trial 1: (a) NeuroCom CoG plot; (b) K1 CoM plot; (c) K2 CoM plot; Trial 2: (d) NeuroCom CoG plot; (e) K1 CoM plot; (f) K2 CoM plot; Trial 3: (g) NeuroCom CoG plot; (h) K1 CoM plot; (i) K2 CoM plot.

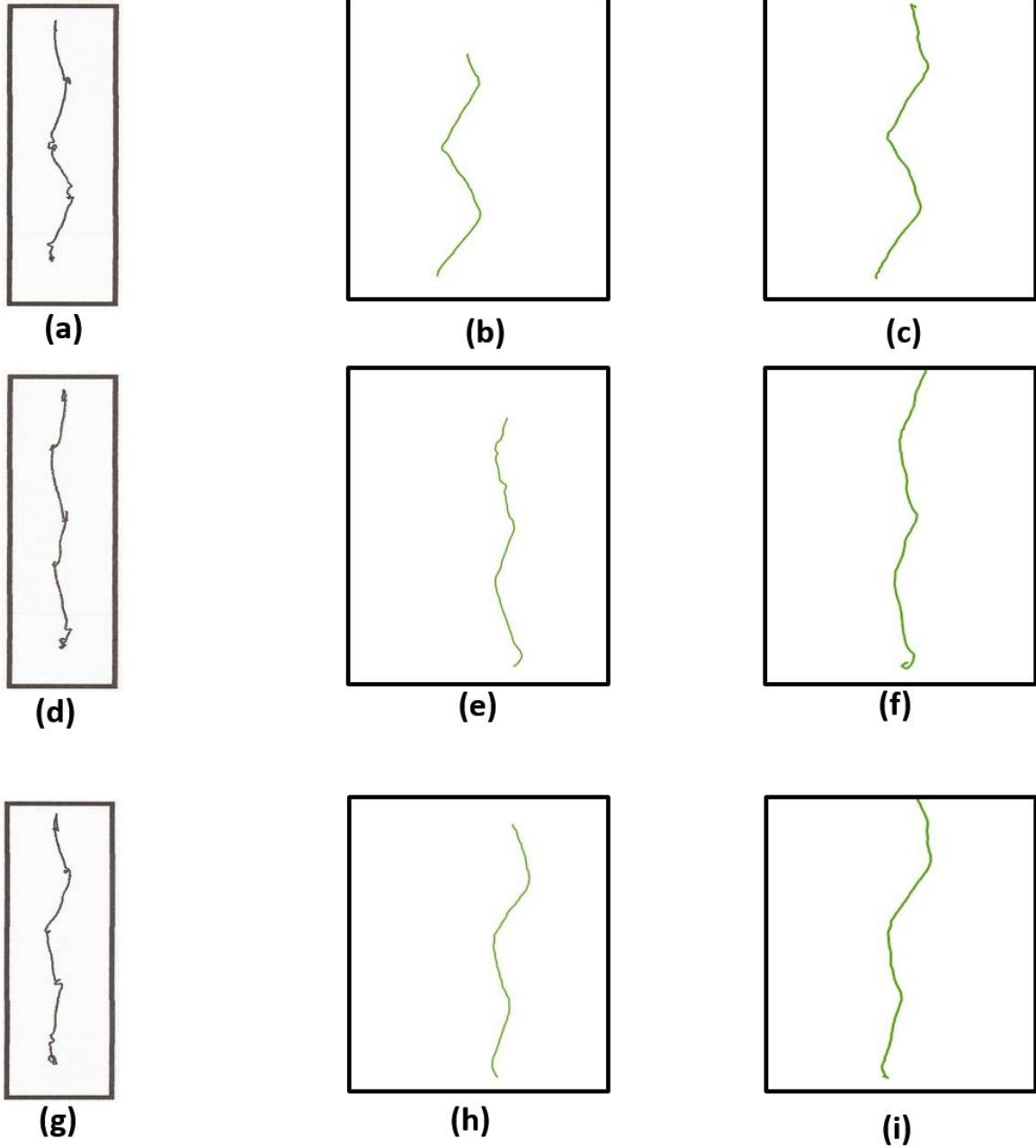


Figure 39 Subject 4- TW eyes open test results. Trial 1: (a) NeuroCom CoG plot; (b) K1 CoM plot; (c) K2 CoM plot; Trial 2: (d) NeuroCom CoG plot; (e) K1 CoM plot; (f) K2 CoM plot; Trial 3: (g) NeuroCom CoG plot; (h) K1 CoM plot; (i) K2 CoM plot.

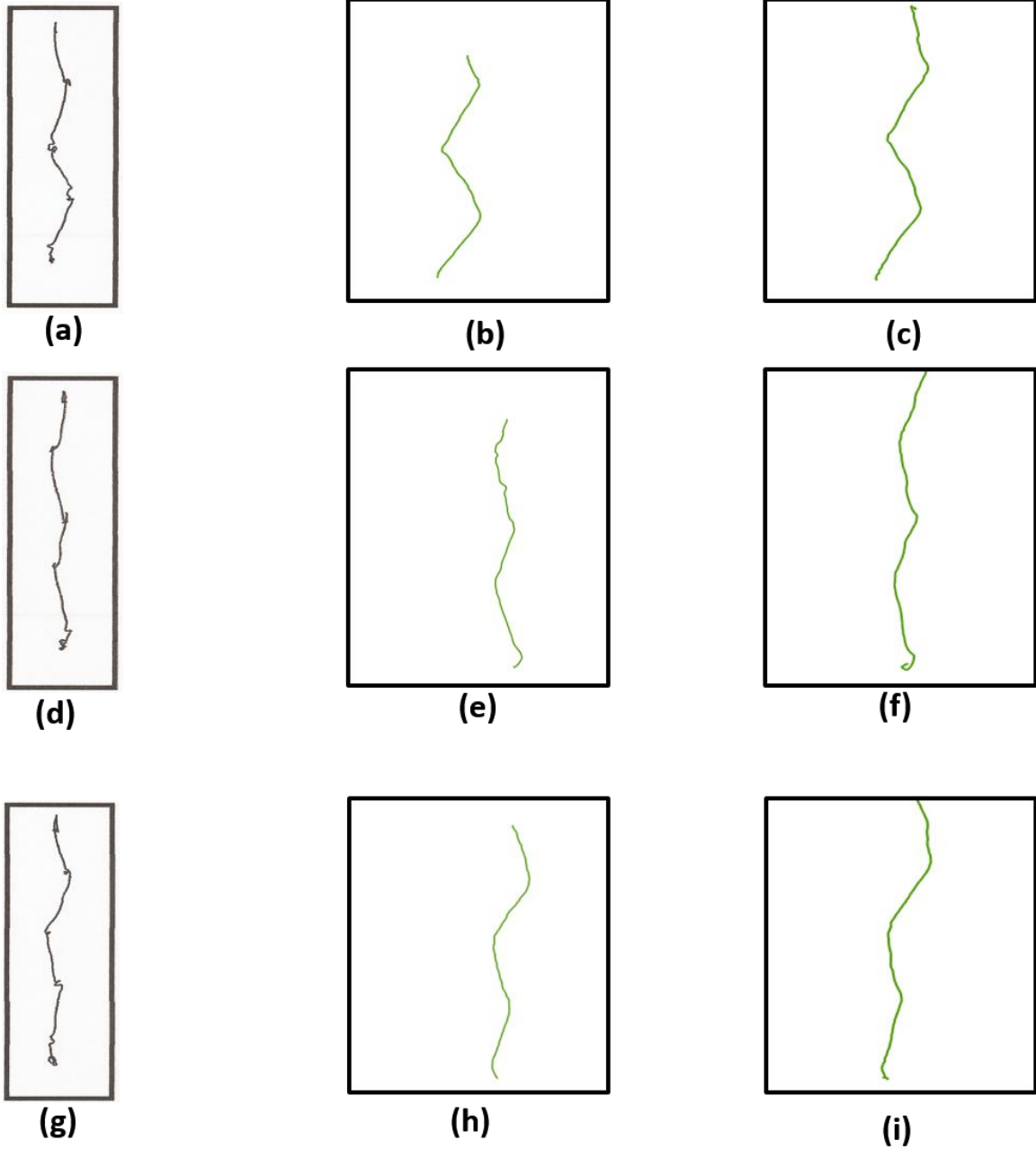


Figure 40 Subject 4- TW eyes closed test results. Trial 1: (a) NeuroCom CoG plot; (b) K1 CoM plot; (c) K2 CoM plot; Trial 2: (d) NeuroCom CoG plot; (e) K1 CoM plot; (f) K2 CoM plot; Trial 3: (g) NeuroCom CoG plot; (h) K1 CoM plot; (i) K2 CoM plot.

## Appendix B

### Code and Data Repository

The code are available at:

- [kronos.cirl.missouri.edu:/home/shared/Git/CenterOfMassKinect1.8.git](https://kronos.cirl.missouri.edu/home/shared/Git/CenterOfMassKinect1.8.git)
- [kronos.cirl.missouri.edu:/home/shared/Git/CenterOfMassKinect2.0.git](https://kronos.cirl.missouri.edu/home/shared/Git/CenterOfMassKinect2.0.git)
- [kronos.cirl.missouri.edu:/home/shared/Git/PTKinectTherapist.git](https://kronos.cirl.missouri.edu/home/shared/Git/PTKinectTherapist.git)
- [kronos.cirl.missouri.edu:/home/shared/Git/PTKinectClient.git](https://kronos.cirl.missouri.edu/home/shared/Git/PTKinectClient.git)

The data are available at:

- [nfs.isilon.rnet.missouri.edu:/ifs/cirl/projectdata/ptkinect/](https://nfs.isilon.rnet.missouri.edu:/ifs/cirl/projectdata/ptkinect/)